machines

Review

Review of Numerical Analysis of Dielectric Barrier Discharge Plasma Actuators for Aircraft Active Flow Control

Jean Fulbert Ituna Yudonago [1], Víctor Martínez Calzada [2,*], Alonso Saldaña Heredia [3], José Luis Rodríguez Muñoz [4] and Adriana Rodríguez Torres [1]

[1] Ingeniería Aeronáutica, Universidad Politécnica Metropolitana de Hidalgo, Boulevard Acceso a Tolcayuca 1009, Tolcayuca 43860, Hidalgo, Mexico; jituna@upmh.edu.mx (J.F.I.Y.); adrodriguez@upmh.edu.mx (A.R.T.)
[2] Departamento de Ingeniería Mecánica, Tecnológico Nacional de México, Instituto Tecnológico de La Laguna, Av. Revolución s/n, Torreón 27000, Coahuila, Mexico
[3] Centro de Investigación en Ingeniería y Ciencias Aplicadas, Universidad Autónoma del Estado de Morelos, Av. Universidad No. 1001, Cuernavaca 62209, Morelos, Mexico; alonso.saldana@uaem.mx
[4] Ingeniería Mecánica, Escuela Superior de Ciudad Sahagún, Universidad Autónoma del Estado de Hidalgo, Carretera Cd. Sahagún-Otumba s/n, Zona Industrial, Ciudad Sahagún CP 43998, Hidalgo, Mexico; jose_rodriguez@uaeh.edu.mx
* Correspondence: vmartinezc@lalaguna.tecnm.mx

Abstract

This paper reviews numerical modeling approaches for Dielectric Barrier Discharge (DBD) plasma actuators in aircraft active flow control. While extensive experimental studies exist, a dedicated review of computational methodologies—covering macroscopic, microscopic, and empirical models—has been absent. This work systematically evaluates major models (Shyy, Suzen–Huang, Dorr–Kloker, Roth, Orlov–Corke, Massines), discussing their formulations, assumptions, computational cost, and applicability. It synthesizes simulation studies in aerodynamic applications such as separation control, drag reduction, transition delay, film cooling, and compressor stability. Key findings show that macroscopic models offer a practical balance between accuracy and cost for design-oriented studies, whereas microscopic models provide deeper physical insight at higher expense. The review highlights the effectiveness of DBD actuators in modifying boundary layers, delaying stall, and improving aerodynamic efficiency. Finally, persistent challenges are identified—including energy efficiency, scalability, and model calibration and future directions are suggested, such as hybrid modeling, multi-actuator arrays, and real-time control integration.

Keywords: Dielectric Barrier Discharge (DBD); plasma actuators; numerical modeling; active flow control

Check for updates

Academic Editor: Davide Lengani

Received: 7 June 2026
Revised: 18 July 2026
Accepted: 23 July 2026
Published: 30 July 2026

1. Introduction

The continuous pursuit of higher aerodynamic efficiency, reduced fuel consumption, and lower emissions has driven the development of advanced aircraft flow control technologies. Conventional flight control systems, based on movable aerodynamic surfaces actuated by hydraulic, pneumatic, electromechanical, or fly-by-wire systems, have undergone remarkable technological evolution over the past decades [1–41]. Although these technologies have significantly improved aircraft controllability and reliability, they still rely on mechanical components that increase system complexity, weight, maintenance requirements, and energy consumption. Consequently, considerable research efforts have been devoted to the development of alternative flow-control techniques capable of improving aerodynamic performance while minimizing mechanical complexity.

Among these alternatives, Active Flow Control (AFC) has emerged as one of themost promising technologies for future aircraft. Unlike conventional control systems, AFC manipulates the boundary layer directly by introducing momentum into the flow without requiring large movable surfaces. This capability enables the control of boundary-layer separation, the delay of stall, drag reduction, lift enhancement, transition control, vortex manipulation, and an improvement in overall aerodynamic efficiency.

Within the field of Active Flow Control (AFC), Dielectric Barrier Discharge (DBD) plasma actuators have attracted particular attention because of their simple construction, rapid response, absence of moving parts, low weight, and ease of integration into aerodynamic surfaces [42,43]. A DBD plasma actuator consists of two asymmetric electrodes separated by a dielectric material and supplied with high-voltage alternating current. The plasma generated around the exposed electrode produces an electrohydrodynamic body force that transfers momentum from the ionized gas to the surrounding neutral air. Numerous experimental investigations have demonstrated their effectiveness for delaying flow separation, increasing lift, reducing drag, suppressing vortex shedding, improving compressor stability, and complementing conventional control surfaces [43–62]. The rapid growth of DBD plasma actuator research has been accompanied by extensive use of Computational Fluid Dynamics (CFD). Numerical simulations provide detailed information about plasma-flow interaction while reducing experimental costs. Consequently, numerous macroscopic, microscopic, and empirical numerical models have been proposed, each presenting different assumptions, computational costs, and predictive capabilities.

Several review papers have addressed different aspects of dielectric barrier discharge (DBD) plasma actuators from experimental, theoretical, and numerical perspectives. Jayaraman and Shyy [63] presented a comprehensive review of plasma-induced fluid dynamics and heat transfer, emphasizing the fundamental physical mechanisms governing electrohydrodynamic (EHD) flow generation, plasma–flow interactions, and heat transfer enhancement in engineering applications. Corke et al. [64] reviewed the operating principles, physical characteristics, actuator configurations, and aerodynamic applications of single DBD plasma actuators, providing one of the earliest comprehensive discussions on plasma actuator physics and modeling strategies for flow control. Cho and Shyy [65] focused primarily on numerical simulations of plasma-based feedback flow control, discussing the implementation of plasma actuator models in Computational Fluid Dynamics (CFD) solvers and their application to low-Reynolds-number aerodynamic flows.

More recently, Wang et al. [62] reviewed the technological development of various plasma actuator configurations, including conventional DBD actuators, synthetic plasma jets, plasma spark jets, three-dimensional plasma actuators, and plasma vortex generators, highlighting their performance in aerodynamic flow control and propulsion-related applications. Portugal et al. [66] summarized more than two decades of research on DBD plasma actuators, covering actuator design, discharge physics, experimental characterization, power consumption, and representative engineering applications. In contrast, Zhang et al. [67] concentrated on the thermal behavior of sinusoidally driven DBD plasma actuators, reviewing heat generation mechanisms, thermal diagnostics, and the influence of operating conditions on actuator performance.

Although these review articles provide valuable insights into the development and application of DBD plasma actuators, their primary emphasis is placed on actuator design, discharge physics, experimental investigations, or general plasma-based flow control. Numerical modeling is generally discussed only as one component of broader reviews, often without a detailed comparison of the available computational methodologies. Consequently, important aspects such as the mathematical formulation of the governing equations, electrohydrodynamic body-force models, charge transport equations, coupling strategies with fluid flow solvers, computational requirements, numerical accuracy, convergence behavior, and applicability to different aerodynamic problems remain scattered throughout the literature. To the best of the authors' knowledge, there is currently no review paper specifically devoted to the numerical modeling methodologies of DBD plasma actuators for aircraft active flow control. The absence of a comprehensive comparison of macroscopic, microscopic, and empirical models makes it difficult for researchers to identify the most appropriate modeling approach for a given aerodynamic application. This review addresses that gap by systematically analyzing the assumptions, mathematical formulations, computational complexity, advantages, limitations, and representative applications of the principal numerical models reported in the literature while also identifying current challenges and future research directions in plasma-assisted active flow control.

The remainder of this review paper is organized as follows. Section 1 introduces the background, motivation, and objectives of the review. Section 2 provides a comprehensive overview of the principal mathematical models developed for DBD plasma actuators. Section 3 reviews the numerical and experimental studies reported in the literature, highlighting their main findings and applications in active flow control. Finally, Section 4 presents the main conclusions and discusses future research directions.

2. Numerical Models for the Design of DBD Plasma Actuators

2.1. Classification of DBD Plasma Actuator Numerical Models

The multitude of parameters involved in the experimental design of the DBD plasma actuator, as well as the high material costs, have motivated the use of CFD as a tool in the design process. There are two main types of numerical models in the literature used for the design of DBD plasma actuators, namely macroscopic models and microscopic models, see Figure 1.

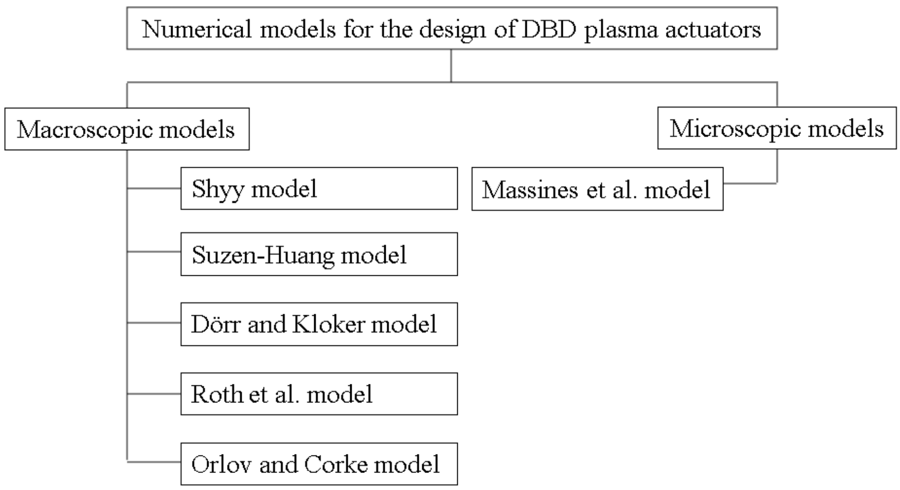

Figure 1. Classification of DBD plasma actuator numerical models.

2.2. Macroscopic Models

Macroscopic models allow for simulating the characteristics of the electric potential and defining the charge density that forms the force created by the DBD plasma actuator. The use of these models also allows for studying the range of required magnitudes of momentum and energy delivered to the flow field near the airfoil wall boundary.

2.2.1. Shyy Model

The Shyy model is one of the simplest models for numerically modeling DBD Plasma actuators [68]. In this model, it is assumed that the electric field (E) has its maximum value at the edge of the upper electrode and its intensity decreases linearly with the distance between the upper electrode and the dielectric surface as shown in Figure 2, where a denotes the height and b denotes the length of the electric field, d is the separation between the two electrodes in the direction x, and the A–B line constitutes the plasma boundary.

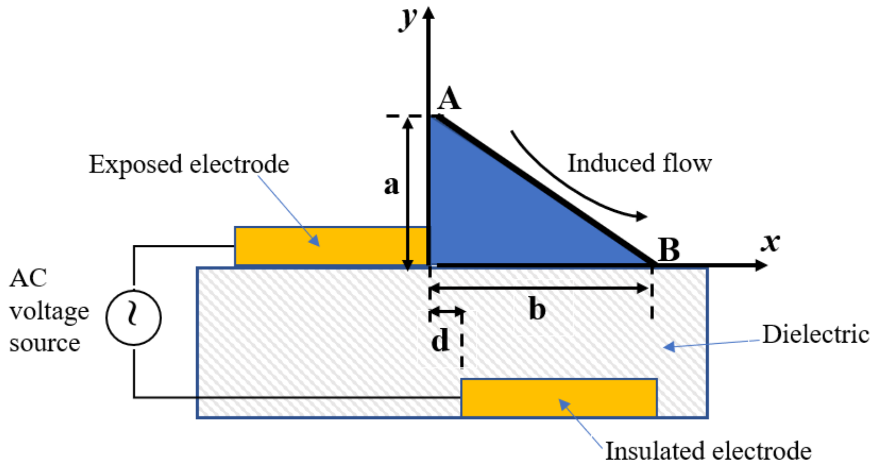

Figure 2. Diagram of a DBD plasma actuator with linear distribution of the electric field in Shyy's model.

For this model, the charge density is assumed to be constant and the variation of the electric field is given by the Equation (1):

$$E(x, y) = |E| = E_0 - k_1 \cdot x - k_2 \cdot y \tag{1}$$

where E_0 is the initial electric field, expressed in $[V/m]$) and defined as:

$$E_0 = \frac{U_0}{d} \tag{2}$$

where U_0 is the applied voltage. The constants k_1 and k_2 are evaluated by the expression (3) by the condition that the local electric field intensity must be equal to the breakdown electric field intensity.

$$\left.\begin{aligned} k_1 &= \frac{E_0 - E_b}{b} \\ k_2 &= \frac{E_0 - E_b}{a} \end{aligned}\right\} \tag{3}$$

In these two equations, the constants k_1 and k_2 are expressed in $[V/m^2]$, and E_b is the intensity of the breakdown electric field, expressed in $[V/m]$ and estimated according to Shyy and Andersson [68] at $3.0 \times 10^6\ V/m$. However, a better estimate of the value of E_b for an atmospheric discharge can be obtained by considering the empirical formula of Peek's law expressed in Equation (4), which was originally developed for corona discharges but has been shown to be applicable to DBD actuators [69,70].

$$E_b = E_a \delta \epsilon \left(1 + \frac{0.308}{\sqrt{0.5 \delta t_u}}\right) \tag{4}$$

where $E_a = 3.1 \times 10^6\ V/m$ is the dielectric strength of air, t_u is the thickness of the top electrode, ϵ is a surface roughness factor equal to 1 for smooth surfaces, and δ is the relative atmospheric density factor defined by Equation (5):

$$\delta = \frac{298p}{T} \tag{5}$$

where T is the temperature in Kelvin, and p is the atmospheric pressure. The value of $\delta = 1$ for air under standard conditions.

The components of the body force along the x and y directions (f_x and f_y) are calculated as:

$$\left.\begin{aligned} f_x &= E_x \rho_c e_c \\ f_y &= E_y \rho_c e_c \end{aligned}\right\} \tag{6}$$

where ρ_c [C/cu.m] is the charge density, $e_c = 1.602 \times 10^{-19}$ C is the charge of an electron, and E_x and E_y are the electric field components in the x and y directions, respectively, which are calculated using the following expressions:

$$\left.\begin{aligned} E_x &= \frac{Ek_2}{\sqrt{k_1^2 + k_2^2}} \\ E_y &= \frac{Ek_1}{\sqrt{k_1^2 + k_2^2}} \end{aligned}\right\} \tag{7}$$

This body force acts only in the regions where plasma is present, which is determined by the field strength at the point.

The components of the effective force on the neutral molecules along the x and y directions (f_{effx} and f_{effy}) are given by:

$$\left.\begin{aligned} f_{effx} &= \alpha f_x \delta \\ f_{effy} &= \alpha f_y \delta \end{aligned}\right\} \tag{8}$$

where α is a factor to account for collision efficiency. The components of the effective force act only during the time Δt during which plasma is formed, which corresponds to one half cycle. According to Shyy et al. [68], this force during the second half of the cycle can be neglected since it has little or no plasma formation. Therefore, this force can be time-averaged over a full cycle, as expressed in Equation (9).

$$\left.\begin{aligned} F_{tavex} &= \frac{f_{effx} \Delta t}{T_t} \\ F_{tavey} &= \frac{f_{effy} \Delta t}{T_t} \end{aligned}\right\} \tag{9}$$

Although the actual electric field distribution in DBD plasma actuators exhibits strong spatial and temporal variations, the linear approximation adopted by Shyy et al. [68] provides an effective representation of the net electrohydrodynamic forcing and has been widely employed due to its reduced computational cost and reasonable agreement with experimentally measured flow characteristics.

2.2.2. Suzen–Huang Model

The Suzen–Huang plasma actuator model is rooted in the concept of electroosmotic flow introduced by D. C. Henry (1931) [71]. This model is rooted in the concept of electroosmotic flow. Electroosmotic flow refers to the motion of a fluid induced by the presence of an applied voltage in a capillary tube or narrow channel.

The mathematical equation that describes electroosmotic flow dimensionally is based on the division of the total electrical potential (Φ) into two parts for weakly ionized gas particles: the first is the potential due to the external electric field (ϕ), and the second part is the electric potential due to the net charge density (φ) [72–76].

$$\Phi = \phi + \varphi \tag{10}$$

These two electric potential terms are related to the relative permittivity of both the medium (ϵ_r) and free space (ϵ_0) through the following equations:

$$\nabla \cdot (\epsilon_r \nabla \phi) = 0 \tag{11}$$

$$\nabla \cdot (\epsilon_r \nabla \varphi) = -\left(\frac{\rho_c}{\epsilon_0}\right) \tag{12}$$

where ρ_c (C/m^3) is the electric charge density, ϵ_r and ϵ_o have units of F/m (farads per meter).

The net charge density (ρ_c) can be defined as the difference between the net positive charge produced by the ions and the net positive or negative charge of the electrons [76,77].

$$\rho_c = e(n_i - n_e) \tag{13}$$

where e is the electric charge of an electron (C) ($e = 1.6 \times 10^{-19}$ C) [73], n_i is the ion density $(1/m^3)$ and n_e is the electron density $(1/m^3)$.

The values of n_i and n_e can be approximated using the Boltzmann relation for the electron and positive ion densities in thermal equilibrium as expressed in Equations (14) and (15) [73,76,78].

$$n_e = n_0 \, exp\left(\frac{e\,\Phi}{kT_e}\right) \tag{14}$$

$$n_i = n_0 \, exp\left(\frac{-e\,\Phi}{kT_i}\right) \tag{15}$$

where n_0 is the plasma density $(1/m^3)$, k is the Boltzmann constant ($k = 1.38 \times 10^{-23}$ m^2kg/s^2K, and T_e and T_i are the temperatures (in Kelvin) of electrons and ions, respectively.

Substituting Equations (14) and (15) into (13) yields a new expression (Equation (16)) for the net charge density as a function of the total electric potential (Φ):

$$\rho_c = e \, n_0 \left[exp\left(\frac{-e\,\Phi}{kT_i}\right) - n_0 \, exp\left(\frac{e\,\Phi}{kT_e}\right) \right] \tag{16}$$

Developing the exponential functions in Equation (16) with the Taylor series in the case of $e\Phi \ll kT$, we obtain:

$$\rho_c = -e^2 \, n_0 \left[\frac{1}{kT_i} + \frac{1}{kT_e} \right] \Phi \tag{17}$$

The Suzen–Huang model can be developed dimensionally or non-dimensionally.

Dimensional Form of Suzen–Huang model

The dimensional form of the Suzen–Huang model is based on the Debye-Huckel approximation, where the electric potential due to the net charge density (φ) has negligible effects in the computational domain of the plasma actuator when the Debye lengths are low [76].

When a high-voltage alternating current is supplied to the electrodes (as shown in Figure 2), the air in their vicinity becomes weakly ionized. This can give rise to magnetohydrodynamic and electrohydrodynamic body forces acting on the external flow and thus inducing stationary or transient velocity components. These body forces are calculated from the Lorentz equation, which can be written as:

$$\vec{F}_b = \rho_c(\vec{E} + (\vec{u} \times \vec{B})) \tag{18}$$

where $\vec{F}_b$ is the body force vector per unit volume (N/m^3) called the Lorentz body force, $\vec{E}$ is the electric field (V/m), $\vec{B}$ is the magnetic field (T), and $\vec{u}$ is the flow velocity vector (m/s).

The Lorentz body force is derived from Maxwell's equations, which are known as Gauss's law for the electric field, Gauss's law for the magnetic field, Faraday's law of electromagnetic induction, and Ampère's law with Maxwell's correction.

- Gauss's law for the electric field:

$$\nabla \cdot \vec{E} = \frac{\rho_c}{\epsilon_0} \tag{19}$$

- Gauss's law for the magnetic field:

$$\nabla \cdot \vec{B} = 0 \tag{20}$$

- Maxwell-Faraday Law:

$$\nabla \times \vec{E} = -\frac{\partial \vec{B}}{\partial t} \tag{21}$$

- Ampere's law with Maxwell's correction:

$$\nabla \times \vec{B} = \mu_0 \vec{J} + \mu_0 \epsilon_0 \frac{\partial \vec{E}}{\partial t} \tag{22}$$

where μ_0 is the permeability of free space (N/A^2), and $\vec{J}$ is the induced current (A/m).

In the case of a quasi-stationary system, $\vec{J}$ and $\vec{B}$ are equal to zero. Furthermore, the time derivatives $\partial\vec{B}/\partial t$ and $\partial\vec{E}/\partial t$ are also equal to zero [71]. Therefore, only Gauss's law for the electric field remains (Equation (19)). This implies that the Lorentz Equation (18) reduces to:

$$\vec{F}_b = \rho_c \vec{E} \tag{23}$$

On the other hand, the electric field can be derived from the gradient of a scalar potential as follows [71,77,79]:

$$\vec{E} = -\nabla\phi \tag{24}$$

Substituting Equation (24) into Equation (23) leads to the expression (25) for the Lorentz body force in terms of the electric potential:

$$\vec{F}_b = \rho_c(-\nabla\phi) \tag{25}$$

https://doi.org/10.3390/machines14080861

Eventually, the Lorentz body force can be added as a source term to the Navier–Stokes equations to obtain the governing equation (Equation (26)) of the computational model of the plasma actuator.

$$\rho\frac{\partial\vec{u}}{\partial t}+\rho(\vec{u}\cdot\nabla)\vec{u}+\nabla P-\nabla(\eta\nabla\vec{u})=\vec{F}_b \tag{26}$$

where ρ refers to the plasma density, η is its dynamic viscosity, $\vec{u}$ is the velocity vector, P is the pressure, and t is the time.

Since the number of variables in Equation (26) is greater than the number of equations, solving the computational model of the plasma actuator is only possible if the mass conservation equation (Equation (27)) is added.

$$\frac{\partial\rho}{\partial t}+\nabla\cdot(\rho\vec{u})=0 \tag{27}$$

Solving Equations (26) and (27) requires establishing boundary conditions in the computational domain. To do this, Equation (11) is solved to determine the electric potential as boundary conditions applied to the electrodes.

Since the electric potential is neglected in the development of the Suzen–Huang dimensional model due to the net charge density (φ), expressed by Equation (12), an additional governing equation is required to determine the net charge density supplied as boundary conditions in the computational domain of the actuator.

This governing equation is derived from two equations, including Equation (12), which is the partial differential equation for the potential due to the net charge density, and Equation (28), which is the equation for the electric charge density expressed in terms of the total electric potential and the Debye length (λ_D) [79].

$$\frac{\rho_c}{\epsilon_0}=-\frac{\Phi}{\lambda_D^2} \tag{28}$$

Since $\Phi=\phi+\varphi$, Equation (28) can be rewritten as:

$$\frac{\rho_c}{\epsilon_0}=-\frac{\phi+\varphi}{\lambda_D^2} \tag{29}$$

Solving φ from Equation (29) gives:

$$\varphi=-\left(\phi+\frac{\rho_c\lambda_D^2}{\epsilon_0}\right) \tag{30}$$

Substituting (30) into (12) gives:

$$\nabla\left(\epsilon_r\nabla\left(\phi+\frac{\rho_c\lambda_D^2}{\epsilon_0}\right)\right)=\frac{\rho_c}{\epsilon_0} \tag{31}$$

which can be expanded as follows:

$$\nabla(\epsilon_r\nabla\phi)+\left(\frac{\epsilon_r\nabla\rho_c\lambda_D^2}{\epsilon_0}\right)=\frac{\rho_c}{\epsilon_0} \tag{32}$$

The first term ($\nabla(\epsilon_r\nabla\phi)$) of Equation (32) is zero, so it can be rewritten as:

$$\nabla\cdot(\epsilon_r\nabla\rho_c)=\frac{\rho_c}{\lambda_D^2} \tag{33}$$

Equation (33) is the second governing equation that, when solved, allows determining the net charge density supplied as boundary conditions in the computational domain of the actuator.

Note that the Debye length is the characteristic length of electrostatic shielding in plasma. Basically, the Debye length determines whether or not body forces come into play in the computational analysis of the plasma actuator [76]. This length can be determined by substituting Equation (28) into Equation (17) as shown in Equation (34) [73,76,78].

$$\lambda_D = \left[\frac{e^2\, n_0}{\epsilon_0}\left(\frac{1}{kT_i} + \frac{1}{kT_e}\right)\right]^{-1/2} \tag{34}$$

The boundary conditions for electric potential and net charge density are described in Figures 3 and 4, respectively.

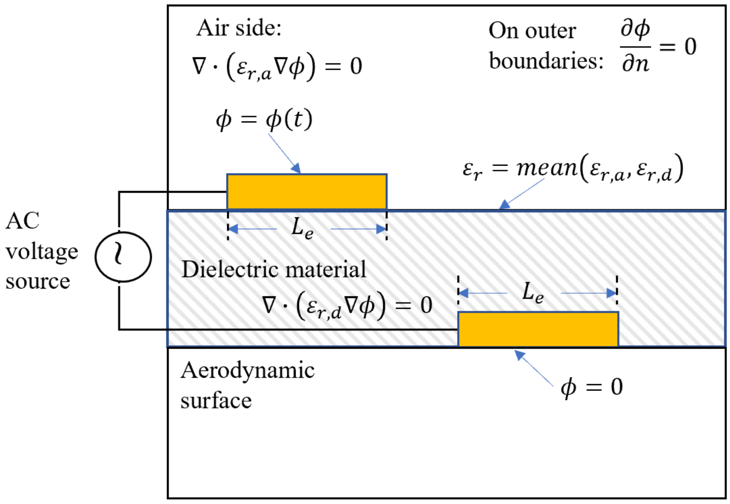

Figure 3. Electric potential boundary conditions over the computational domain of the actuator using the Suzen–Huang model.

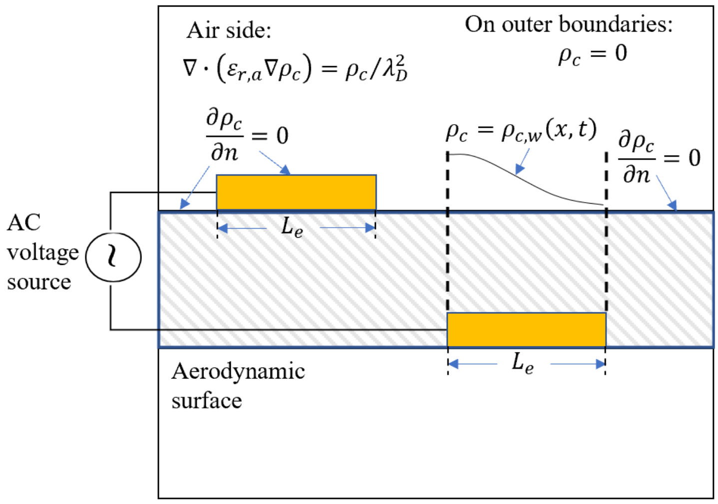

Figure 4. Electric charge density boundary conditions over the computational domain of the actuator using the Suzen–Huang model.

As can be seen in Figure 3, a zero normal gradient ($\partial\phi/\partial n$) is imposed for the electric potential at the outer boundaries of the computational domain. The exposed (top) electrode has an electric potential greater than zero, which can vary with time, while the isolated electrode is prescribed as ground with an electric potential equal to zero. In the wall of the region covering the isolated electrode, a relative permittivity is considered, which is the average of the relative permittivity of air ($\epsilon_{r,a}$) and dielectric material ($\epsilon_{r,d}$). In Figure 4, a zero normal gradient ($\partial\rho_c/\partial n$) is imposed for the electric charge density on the solid walls, except for the region that covers the isolated electrode, and the charge density is set to zero at the outer limits. Downstream of the exposed electrode, in the region above the insulated electrode, the electric charge density is prescribed so that it synchronizes with the time variation of the applied voltage $\phi(t)$ at the exposed electrode, as described in the following equation [71]:

$$\rho_{c,w}(x,t) = \rho_c^{max} G(t) f(t) \tag{35}$$

where ρ_c^{max} (C/m^3) is the maximum value of the electric charge density supplied in the domain, and $f(t)$ is the waveform function that can be a sinusoidal wave given by [71]:

$$f(t) = sin(2\pi\omega t) \tag{36}$$

where ω (Hz) refers to the frequency of the supplied AC voltage.

When $f(t)$ is a square wave, it is given by:

$$f(t) = \begin{cases} 1 & \text{for } sin(2\pi\omega t) \geq 0 \\ -1 & \text{for } sin(2\pi\omega t) < 0 \end{cases} \tag{37}$$

On the other hand, $G(t)$ in Equation (35), is a function that can be chosen to resemble the plasma distribution over the insulated electrode [71]. Experimental results suggest that this distribution is similar to a Gaussian mean distribution given by:

$$G(t) = exp[-(x-\mu)^2/(2\sigma^2)], \text{ for } x \geq 0 \tag{38}$$

where μ is the location parameter indicating the x position of the maximum, and σ is a scale parameter determining the decay rate. The effect of σ (defined in terms of the electrode length, L_e) on the behavior of $G(t)$ can be observed in [80–82], where representative plots are shown for various values of this parameter (with $\mu = 0$); in those plots, it is evident that as σ increases, the decay rate decreases.

Non-Dimensional Form of the Suzen–Huang Model

The non-dimensional form of the Suzen–Huang model was developed by Ibrahim and Skote [74,76,77] to transform the original Suzen–Huang equations into non-dimensional form to simplify calculations and provide a more general understanding of plasma actuator behavior. The transformation involves the introduction of dimensionless variables based on the characteristic length, electric field, and charge density, according to research studies.

The modification is specifically based on Equations (11) and (33), which are rewritten in non-dimensional form as shown in Equations (39) and (40):

$$\nabla \cdot (\epsilon_r \nabla \overset{*}{\phi}) = 0 \tag{39}$$

$$\nabla \cdot (\epsilon_r \nabla \overset{*}{\rho}_c) = \frac{\overset{*}{\rho}_c}{\lambda_D^2} \tag{40}$$

where

$$\overset{*}{\phi} = \frac{\phi}{\phi_0(\tau)} \tag{41}$$

$$\overset{*}{\rho_c} = \frac{\rho_c}{\rho_{c,0}(\tau)} \quad (42)$$

where τ is a dimensionless amount of time, which is related to frequency as:

$$\tau = \omega t \quad (43)$$

The term ϕ_0 (V) is the AC voltage applied to the upper (exposed) electrode. It is calculated using the following formula:

$$\phi_0(\tau) = \phi_{max} \times f(\tau) \quad (44)$$

where ϕ_{max} (V) is the maximum amplitude of the supplied AC voltage, and $f(\tau)$ is the function for the AC voltage source, expressed as follows:

$$f(\tau) = sin\left(\frac{\pi}{2}\tau\right) \quad (45)$$

The term $\rho_{c,0}$ is the net charge density established as a boundary condition at the lower (insulated) electrode. It is calculated using the following formula:

$$\rho_{c,0}(\tau) = \rho_{c,max} \times f(\tau) \quad (46)$$

where $\rho_{c,max}$ (C/m^3) is the maximum electric charge density of the alternating current supplied.

The electric potential boundary conditions and net charge density for the non-dimensional form of the Suzen–Huang model are described in Figure 5 and Figure 6, respectively.

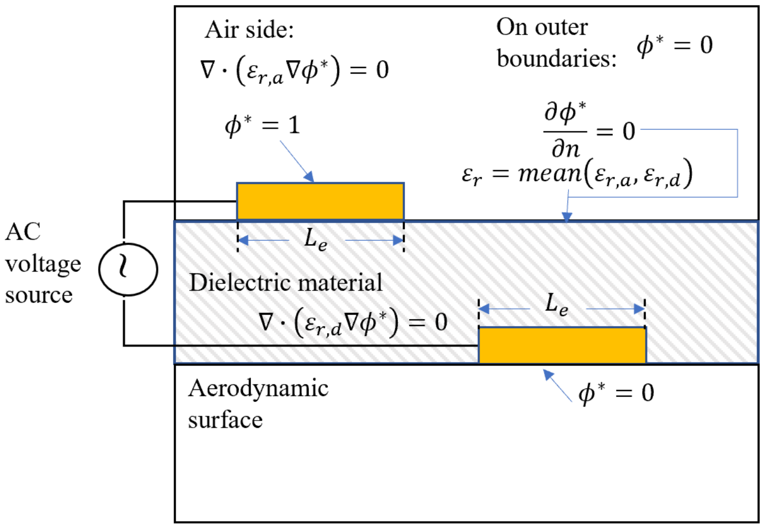

Figure 5. Non-dimensional electric potential boundary conditions over the computational domain of the actuator using the Suzen–Huang model.

In Figure 5, the boundary condition $\overset{*}{\phi}$ for the upper (exposed) electrode is equal to one, so that once $\overset{*}{\phi}$ is determined, the dimensional value ϕ in Equation (41) can be obtained at any given time by multiplying $\overset{*}{\phi}$ with the value corresponding to $\phi_0(\tau)$ calculated by Equation (44).

Similarly, in Figure 6, the boundary condition $\overset{*}{\rho_c}$ for the lower (insulated) electrode is equal to one. This allows the dimensional value ρ_c in Equation (42) to be obtained by multiplying $\overset{*}{\rho_c}$ with the corresponding value for $\rho_{c,0}(\tau)$ calculated by Equation (46).

The governing Equations (39) and (40) are used to determine the dimensionless Lorentz body force ($\overset{*}{F_b}$). These equations are solved separately from the Navier Stokes equations. Then, the dimensional Lorentz body force ($\vec{F_b}$) can be obtained by multiplying $\overset{*}{F_b}$ with the value corresponding to the product of $\rho_{c,mas}$ and ϕ_{max} as expressed in Equation (47).

$$\overset{*}{F_b} = \frac{\vec{F_b}}{(\rho_{c,max} \times \phi_{max})} \tag{47}$$

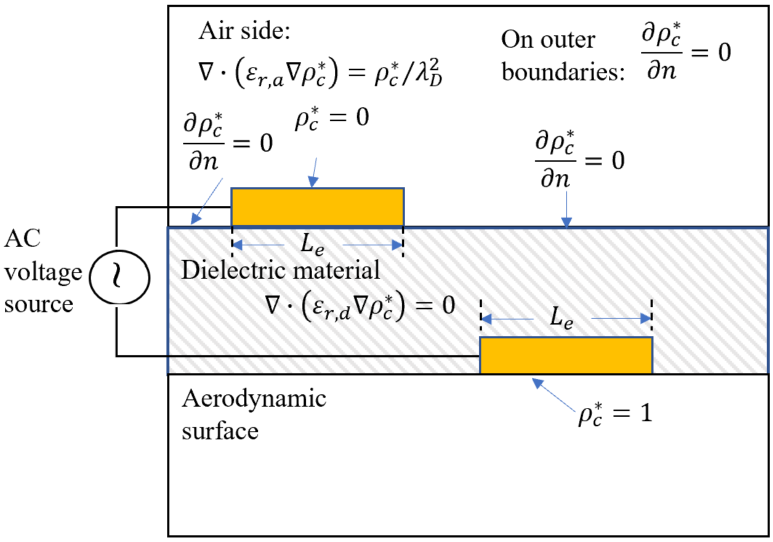

Figure 6. Non-dimensional electric charge density boundary conditions over the computational domain of the actuator using the Suzen–Huang model.

Finally, $\vec{F_b}$ is added as a source term to the Navier–Stokes equations (Equation (26)) and, together with the mass conservation equation (Equation (27)), are used to model the computational domain of the plasma actuator.

Experimental validations have shown that Suzen–Huang-based body-force models can satisfactorily reproduce the global characteristics of DBD-induced flows, including velocity distribution and jet formation. Nevertheless, their predictive accuracy decreases when resolving localized plasma phenomena and instantaneous discharge dynamics.

Modified Suzen–Huang Model

The modifications to the Suzen–Huang model proposed by Ibrahim and Skote [75,77] consist, on the one hand, in changing the boundary conditions applied in the non-dimensional model [74,77] and, on the other hand, in adding an electrode exposed to the upper surface of the dielectric material.

The change of boundary conditions is carried out by replacing the expression $(\partial\phi/\partial n)$ at the boundary above the encapsulated electrode (see Figure 5) by the expression $\nabla_t(\epsilon_{r,m}\lambda_D\nabla_t\overset{*}{\phi})$, where λ_D is the thin layer thickness, $\epsilon_{r,m}$ is the relative apparent permittivity, and the term ∇_t describes the tangential derivative of the non-dimensional electric potential variable. As for the non-dimensional charge density, the original boundary condition at the surface of the encapsulated electrode $(\overset{*}{\rho_c} = 1)$ in Figure 6 is replaced by $(\overset{*}{\rho_c} = 0)$. This modification favors an instantaneous growth of the charge density along the boundary of the encapsulated electrode that propagates in the normal (upward) direction of the dielectric surface. Furthermore, the original boundary condition at the dielectric surface above the encapsulated electrode $(\partial\overset{*}{\rho_c}/\partial n = 0)$ is replaced by a combination of two previous boundary conditions that are $(\partial\overset{*}{\rho_c}/\partial n = 0)$ and $(\overset{*}{\rho_c}/\partial n = 0)$.

2.2.3. Dörr and Kloker Model

Original Form of Dörr and Kloker Model

The Dörr and Kloker model is an empirical model based on a velocity field approach generated by a DBD actuator, which is determined using anemometry techniques such as Particle Image Velocimetry (PIV) or hot wire [69,83]. In this model, the effect of the plasma actuator is determined by a dimensionless, wall-parallel planar force distribution $(\vec{f}_x)$, which is based on the empirical model proposed by Maden et al. [84]. This empirical model was extended in two dimensions using the same formulation to calculate the wall-normal force component $(\vec{f}_y)$. The distribution of the body force vector per unit volume $(N/m3)$ called the corresponding dimensional Lorentz body force $(\vec{f}_b(x,y))$ is calculated by the following formula (Equation (48)):

$$\vec{f}_b(x,y) = f(x,y)\frac{\overline{\rho}_\infty \overline{U}_\infty^2}{L} = f(x,y)\frac{\overline{\rho}_\infty^2 \overline{U}_\infty^3}{Re\overline{\mu}_\infty} \quad (48)$$

where $\overline{\rho}_\infty$ is the air density, $\overline{U}_\infty^2$ is the free stream velocity, L is the reference length, Re is the Reynolds number, $\overline{\mu}_\infty$ is the dynamic viscosity of air and $f(x,y)$ is the dimensionless body force distribution which is expressed by the following empirical formula (Equation (49)) [69]:

$$f(x,y) = c_x\left(a_0a_1x + a_0^2a_2x^2\right)e^{-a_0x}\left(b_1y + b_2y^2\right)e^{-b_0y^{2/5}} \quad (49)$$

The empirical formula for the dimensionless body force distribution can be rewritten as follows:

$$f(x,y) = c_xX(x)Y(y) \quad (50)$$

where $X(x)$ and $Y(y)$ are the dimensionless magnitude of the force along the x and y axis, respectively. Both magnitudes are expressed through the following empirical models (Equation (51)):

$$\begin{aligned} X(x) &= \left(a_0a_1x + a_0^2a_2x^2\right)e^{-a_0x} \\ Y(y) &= \left(b_1y + b_2y^2\right)e^{-b_0y^{2/5}} \end{aligned} \quad (51)$$

where $x, y \geq 0$; $b_0 > 0$; $a_{1,2}, b_{1,2}, c_x \ni \mathbb{R}$. These coefficients allow the force distribution to be controlled, allowing the length and height of the force to be modified.

Modified Form of Dörr and Kloker Model

Bernal-Orozco et al. [69] have shown that the model proposed by Dörr and Kloker may have difficulty in accurately predicting the behavior of a DBD actuator, because the dimensional body force distribution equation does not include operating parameters of a DBD actuator such as voltage and frequency, and also takes into account the free stream velocity, making it invalid in cases with still air, which limits the use of this model. Therefore, Bernal-Orozco et al. [69,85] proposed a modification to the Dörr and Kloker model, which consisted of multiplying the dimensionless body force distribution (Equation (49)) by the dimensional electrohydrodynamic (EHD) force factor, which allows for a better approximation of the force for a given voltage and frequency. In addition to using the aforementioned technique, the coefficient values of the Dörr and Kloker model were modified in order to reduce the length and height of the force.

In general, plasma actuator simulation using the modified Dörr and Kloker model achieves good results and has a low computational cost, but depends on the availability of experimental data for the dimensional factor of the EHD force, which limits its use [69,85].

2.2.4. Roth et al. Model

The model proposed by Roth et al. [86] is one of the oldest macroscopic models. The main difference between this model and the one proposed by Suzen–Huang is that the body force is proportional to half the vacuum permittivity and the square of the electric field, as shown in the following equation (Equation (52)):

$$\vec{F}_b = \frac{1}{2}(\epsilon_0 \vec{E}^2) \tag{52}$$

The main disadvantage of this model is that it can only model a one-dimensional flow, which does not apply to the aerodynamic plasma actuator [76,80].

2.2.5. Orlov and Corke Model

Another macroscopic model prior to the Suzen–Huang model was introduced by Orlov and Corke [87]. The model was designed to model three-dimensional flow. The calculation of the body force per unit volume includes the net electric charge density, the electric field ($\vec{E}$), the permittivity of free space (ϵ_0), the Debye length (λ_D), and the total electric potential (Φ), as shown in the following expression (Equation (53))

$$\vec{F}_b = \rho_c \vec{E} = -\left(\frac{\epsilon_0}{\lambda_D^2}\right)\Phi\vec{E} \tag{53}$$

In this model, the net charge density at any point in the plasma is defined as the difference between the net positive charge produced by the ions and the net negative charge of the electrons, as described in the following equation (Equation (54)).

$$\rho_c = e(n_i - n_e) \tag{54}$$

The net charge density at any point in the plasma can also be defined by the relationship between the total electric potential and the Boltzmann equation, assuming a quasi-steady state with a time scale long enough for the charge store to distribute, as shown in Equation (55).

$$\rho_c \approx -e\, n_0 \left[\frac{e\Phi}{kT_i} + \frac{e\Phi}{kT_e}\right] \tag{55}$$

The model concludes that the net charge density at any point in the plasma is proportional to the potential at that point [76].

Orlov and Corke [87] developed another lumped parameter model to simulate the behavior of the single-dielectric-barrier discharge aerodynamic plasma actuator. The model allows calculating the voltage and current intensity in plasma near a dielectric surface. Both parameters allow evaluating the power consumption of the dielectric barrier discharge plasma actuators $P(t)$, which is calculated by means of the following expression (Equation (56)):

$$P(t) = I_p(t)\left[V_{app}(t) - V_{2A}(t)\right] \tag{56}$$

where $I_p(t)$ is the current intensity in plasma near a dielectric surface, which is proportional to the plasma conductance, G_p, and is given by (Equation (57)):

$$I_p(t) = G_p(t)\left[V_{app}(t) - V_{2A}(t)\right] \tag{57}$$

$G_p(t)$ is proportional to the plasma width as defined in Equation (58):

$$G_p(t) = \left(\frac{G_0}{L}\right)x(t) \tag{58}$$

where L is the length of the actuator, x is the extent of the plasma, G_0 is the conductance of the plasma when the plasma reaches maximum extent at $x = x_{max}$.

$V_{app}(t)$ is the applied voltage defined in terms of its time derivative as follows (Equation (59)):

$$\frac{dV_{app}(t)}{dt} = V_0\omega cos(\omega t) \tag{59}$$

V_0 is the amplitude of the applied voltage, and ω is its angular frequency.

$V_{2A}(t)$ in Equations (56) and (57) is the voltage across the virtual electrode covered by plasma, which is defined in terms of its time derivative by the following governing Equation (60):

$$\frac{dV_{2A}(t)}{dt} = \frac{dV_{app}(t)}{dt}\left(\frac{C_{1A}(t)}{C_{1A}(t) + C_{2A}(t)} + \frac{I_p(t)}{C_{1A}(t) + C_{2A}(t)}\right) \tag{60}$$

C_{1A} represents the capacitance between the exposed electrode and the top surface of the dielectric, while C_{2A} represents the capacitance between the top surface of the dielectric and the encapsulated electrode. Both capacitances are defined as follows:

$$\left.\begin{aligned} C_{1A}(t) &= \alpha C_{2A}(t) \\ C_{2A}(t) &= \frac{\epsilon_0 z x(t)}{d} \end{aligned}\right\} \tag{61}$$

where α is a constant that is estimated from measurements, ϵ_0 is the permittivity of the free space, z is the spanwise length of the actuator, and d is the thickness of the dielectric.

2.3. Microscopic Models

Microscopic models, also called charge transport models, are models used to capture the motion of charged particles in the vicinity of the airfoil wall boundary.

2.3.1. Massines et al. Model

Massines et al. [88] are the pioneers in developing the microscopic model for the design of DBD plasma actuators. The model consists of the coupling of the drift diffusion equation for electrons (Equation (62)) and ions (Equation (63)) and Maxwell's equation (Equation (64)), as described below [76,88–90]:

$$\frac{\partial n_e}{\partial t} + \vec{\nabla}\cdot\left[-n_e\mu_e\vec{E} - D_e\vec{\nabla}n_e\right] = n_e v_i - r n_e n_i \tag{62}$$

$$\frac{\partial n_i}{\partial x} + \vec{\nabla}\cdot\left[-n_i\mu_i\vec{E} - D_i\vec{\nabla}n_i\right] = n_e v_i - r n_e n_i \tag{63}$$

$$\vec{\nabla}\cdot\left(\epsilon\vec{E}\right) = \frac{e}{\epsilon_0}(n_i - n_e) \tag{64}$$

where n_e and n_i are electron and ion densities $(1/m^3)$, μ_e and μ_i are electron and ion mobilities, $(m^2/(sV))$, E is the electric field (V/m), D_e and D_i are diffusion coefficients, v_i is the ionization frequency $(1/s)$, r is the recombination rate (m^3/s), ϵ_0 is the vacuum permittivity (F/m), ϵ is the relative permittivity, and e is the electron charge (C).

The Lorentz body force for the microscopic model is calculated using Equation (65).

$$\vec{F}_b = \rho_c \vec{E} = e(n_i - n_e)\vec{\nabla}\phi \tag{65}$$

where ρ_c is the charge density $(C/m3)$, and ϕ is the electric potential.

The influence of the body force on the airflow is taken into account by including the Lorentz body force in the Navier–Stokes equations (Equation (66)):

$$\begin{gathered} \rho\frac{\partial\vec{u}}{\partial t} + \vec{\nabla}(\eta\vec{\nabla}\vec{u}) + \rho(\vec{u}\cdot\vec{\nabla})\vec{u} + \vec{\nabla}P = e(n_i - n_e)\vec{\nabla}\phi \\ \frac{\partial\rho}{\partial t} + \vec{\nabla}\cdot(\rho\vec{u}) = 0 \end{gathered} \tag{66}$$

In 1998, Massines et al. [88] used this model to experimentally and theoretically study a dielectric-gated atmospheric pressure glow discharge. The theoretical study consisted of a one-dimensional model based on the simultaneous solution of continuity equations for charged and excited particles and Maxwell's equation. The use of these equations laid the groundwork for future microscopic models.

Massines et al. [88] were among the first to use this model to experimentally and theoretically study a dielectric-gated atmospheric pressure glow discharge. The theoretical study consisted of a one-dimensional model based on the simultaneous solution of continuity equations for charged and excited particles and Maxwell's equation. The use of these equations laid the groundwork for future microscopic models.

A few decades later, Boeuf and Pitchford [89] in 2005 performed a similar study to model the electrohydrodynamic forcing and aerodynamic flow acceleration in a dielectric surface discharge barrier considering nitrogen and oxygen at atmospheric pressure. Numerical results showed that this forcing is significant only in the envelope of the surface discharge propagating along the dielectric surface when the cathode is below the dielectric layer. In 2008, Rouffet [90] used Comsol software to investigate the multiphysics approach of a plasma actuator consisting of a mixture of ions, electrons, and neutral molecules by numerical simulations.

The microscopic model has many advantages, as it is suitable for resolving the trajectories of individual charge particles that constitute the charge density. However, its main disadvantage is that it requires high computational resources since its plasma processing time scale is approximately 10^{-8} to $10^{-9}s$, compared to macroscopic models such as the dimensional and non-dimensional Suzen–Huang models whose processing time scale is approximately 10^{-4} s [76].

2.3.2. Evolution over Time of Numerical Models for DBD Plasma Actuators

Figure 7 illustrates the temporal evolution of numerical models for DBD plasma actuators, clearly highlighting the differences between early models and more recent models. The early models, developed in the late 1990s and early 2000s, are characterized by relatively simple formulations, mainly empirical or dimensional, with a limited number of parameters and a simplified representation of plasma effects. These models were useful for gaining an initial understanding of the phenomenon; however, they exhibited limitations in terms of accuracy and general applicability.

In contrast, the new and modified models, developed from around 2010 onward, incorporate non-dimensional formulations and more detailed physical adjustments, leading to an improved representation of the plasma–flow interaction. These advanced versions aim to overcome the limitations of the early models by providing greater numerical robustness, improved stability, and enhanced predictive capability, in line with current requirements for aerodynamic flow simulation and control.

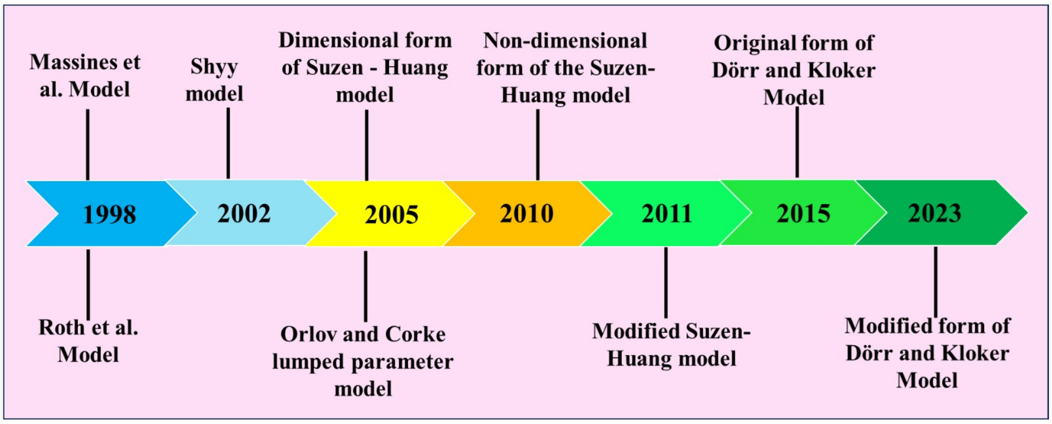

Figure 7. Timeline of numerical model development for DBD plasma actuators [68,69,71,74–77,77,83,86–88].

3. Software for Simulation

3.1. Shyy's Model

Development and validation of the Shyy phenomenological model.

The numerical representation of dielectric barrier discharge (DBD) plasma actuators has evolved considerably over the last two decades, leading to the development of several phenomenological models capable of reproducing the electrohydrodynamic (EHD) body force without explicitly solving the complex plasma chemistry. Among these approaches, the phenomenological model proposed by Shyy et al. [68] has become one of the most widely adopted due to its balance between physical consistency, numerical robustness, and computational efficiency. Instead of resolving the ionization process, the model introduces the plasma-induced force as an additional momentum source within the Navier–Stokes equations, providing an efficient framework for simulating the interaction between plasma discharges and fluid flow.

The original work of Shyy et al. [68] demonstrated that this simplified representation successfully reproduces the wall-jet generated by DBD actuators under atmospheric conditions. Their simulations showed that both the induced jet velocity and the downstream pressure rise increase with the applied voltage and excitation frequency, confirming the capability of plasma actuators to accelerate the near-wall flow. Beyond aerodynamic control, the study also revealed a significant enhancement of convective heat transfer, with local heat fluxes reaching approximately 4.5 times those obtained without plasma actuation. These findings established the foundation for subsequent numerical investigations involving active flow control and thermal management while demonstrating that phenomenological approaches could accurately capture the dominant macroscopic effects of plasma-induced forcing without incurring the computational cost associated with detailed plasma kinetics.

As the use of DBD actuators expanded into increasingly complex aerodynamic configurations, several researchers evaluated the predictive capability of the Shyy model against alternative phenomenological formulations. Among these, the comparison performed by Abdelraouf et al. [91] represents one of the most comprehensive validations available in the literature. The authors compared the Shyy and Suzen formulations for simulating flow separation control over a NACA0012 airfoil, showing that both models produced nearly identical aerodynamic predictions, including a stall delay of approximately two degrees and a lift increase of about 6.1%. Despite these comparable aerodynamic results, the Shyy formulation required substantially fewer iterations and considerably lower computational time, highlighting its superior numerical efficiency. Owing to its straightforward implementation as1a momentum source term and its reduced computational cost, the study concluded that the Shyy model remains the preferred option for large-scale engineering simulations where computational efficiency is a critical consideration.

Collectively, these pioneering studies established the Shyy model as the reference phenomenological formulation for DBD plasma actuator simulations. The combination of satisfactory predictive capability, numerical stability, and ease of implementation has facilitated its widespread adoption in computational fluid dynamics, particularly for applications involving aerodynamic flow control, turbomachinery, and aerothermal systems. Consequently, the vast majority of subsequent investigations have employed this formulation either directly or as the baseline against which newer plasma models are assessed.

Aerodynamic flow control applications.

Following its successful validation, the Shyy phenomenological model rapidly became the preferred numerical framework for investigating the aerodynamic capabilities of dielectric barrier discharge (DBD) plasma actuators. The simplicity of incorporating the plasma-induced body force into the momentum equations has enabled its application to a wide range of active flow control problems, including boundary-layer separation delay, lift enhancement, vortex suppression, shock-wave attenuation, and aeroelastic stabilization. Despite the diversity of these applications, most studies consistently demonstrate that plasma actuation modifies the near-wall momentum distribution, delaying flow separation and improving aerodynamic performance without requiring mechanical moving parts.

Flow separation control over airfoils has received particular attention because of its direct influence on lift generation and stall characteristics. Numerical investigations conducted using the Shyy formulation consistently report that plasma-induced momentum injection energizes the boundary layer, promoting flow attachment and delaying separation under adverse pressure gradients. This behavior has been demonstrated for both steady and unsteady aerodynamic conditions. For example, Abdelraouf et al. [91] showed that DBD actuation delayed the stall angle of a NACA0012 airfoil by approximately two degrees while increasing the maximum lift coefficient by more than 6%. Similar conclusions were obtained by Hasan and Atkinson [92], who investigated the NASA hump configuration as a representative turbulent separation problem. Their large-eddy simulations demonstrated that positioning the plasma actuator immediately upstream of the natural separation point generated sufficient momentum addition to eliminate the separated region almost entirely, highlighting the importance of actuator placement in maximizing control authority.

The influence of plasma actuation has also been investigated under highly unsteady aerodynamic conditions representative of flapping wings and oscillating airfoils. Mahboubidoust et al. [93] demonstrated that actuator location strongly influences the aerodynamic response of an oscillating NACA0012 airfoil operating at low Reynolds numbers. While leading-edge actuation promoted flow attachment, trailing-edge plasma proved considerably more effective in simultaneously increasing lift and reducing drag by modifying vortex shedding during the pitching cycle. Depending on the reduced frequency, lift improvements approaching 30% and drag reductions exceeding 12% were obtained, confirming that plasma actuation remains effective even under strongly time-dependent flow conditions.

As research progressed toward more demanding operating regimes, several studies explored the effectiveness of DBD actuators under higher Reynolds and Mach numbers. Zheng et al. [94] performed one of the most comprehensive comparisons between conventional alternating-current (AC) DBD actuators and nanosecond-pulsed plasma actuators. Their combined numerical and experimental investigation demonstrated that the governing control mechanism depends strongly on the operating conditions. Under low-Reynolds-number conditions, conventional AC actuators primarily improve aerodynamic performance through momentum injection, whereas nanosecond-pulsed actuators generate localized thermal disturbances that become increasingly effective as flow velocity increases. Their results showed that nanosecond actuation completely suppressed flow separation within a few milliseconds while producing substantially larger lift coefficients than conventional AC excitation, indicating that thermal energy deposition becomes the dominant control mechanism in high-speed applications.

Beyond conventional airfoil configurations, the Shyy model has also been successfully applied to more complex three-dimensional aerodynamic problems involving vortex control and shock-wave interactions. Anzalotta et al. [95] investigated the mitigation of tip leakage vortices generated by finite wings using DBD plasma actuators installed inside the wing tip gap. Both numerical simulations and experimental measurements demonstrated that continuous plasma forcing significantly weakened the leakage vortex by generating a stationary counter-rotating structure that opposed the natural leakage flow. The resulting reduction in low-velocity wake regions confirmed the potential of plasma actuation for mitigating vortex-induced aerodynamic losses.

Similarly, Bagheri et al. [96] extended the application of momentum-source concepts to compressible supersonic flows, where plasma-inspired body forces were employed to modify shock-wave/boundary-layer interactions inside a low-aspect-ratio duct. Their simulations revealed that appropriately positioned momentum sources substantially weakened shock intensity, reduced the separation bubble, and smoothed discontinuities within the flow field. Increasing the forcing intensity further improved shock attenuation, demonstrating that body-force-based plasma models remain effective even in highly compressible environments.

The versatility of the Shyy formulation has also enabled its application to aeroelastic control problems, where flow manipulation must remain synchronized with structural motion. De Giorgi et al. [97] investigated alternating-current DBD actuators operating on oscillating compressor cascades and demonstrated that the phase relationship between pressure-side and suction-side actuators governs the resulting aerodynamic damping. An optimal phase difference reduced both lift and pitching moment fluctuations by nearly 50%, substantially increasing aeroelastic stability and mitigating flutter susceptibility. These results illustrate that plasma actuators are capable not only of modifying mean aerodynamic loads but also of controlling the dynamic response of oscillating lifting surfaces.

Collectively, these investigations demonstrate the remarkable versatility of the Shyy phenomenological model across a broad spectrum of aerodynamic applications. Although the specific control mechanisms differ according to the flow regime, a common trend emerges throughout the literature: plasma-induced body forces consistently enhance the near-wall momentum, weaken adverse pressure-gradient effects, suppress coherent vortical structures, and delay or eliminate flow separation. These improvements translate into measurable gains in lift, reductions in drag and aerodynamic losses, enhanced flow stability, and improved aeroelastic behavior. Consequently, the Shyy formulation has evolved from a simplified numerical approximation into one of the most widely accepted computational tools for the design and optimization of plasma-based active flow control strategies.

Applications in Turbomachinery and Aerothermal Systems.

As numerical confidence in the Shyy phenomenological formulation increased, its application gradually expanded beyond conventional aerodynamic flow control toward more complex engineering systems involving rotating machinery and aerothermal management. These applications introduced additional physical challenges, including blade rotation, highly three-dimensional flow structures, periodic aerodynamic loading, and strong fluid–thermal interactions. Nevertheless, the computational efficiency of the Shyy model allowed researchers to investigate these phenomena while preserving an adequate representation of plasma-induced momentum transfer.

One of the earliest extensions of plasma-based flow control to rotating aerodynamic devices focused on cycloidal rotors. Benmoussa et al. [98] incorporated the Shyy body-force formulation into computational fluid dynamics simulations to evaluate the influence of DBD plasma actuators on the unsteady aerodynamics of a six-bladed cycloidal rotor. Unlike previous investigations devoted primarily to geometric optimization, this work introduced active plasma control as a complementary strategy for improving rotor performance. By synchronizing actuator activation with the azimuthal position of each blade, the authors proposed a control methodology capable of generating a "virtual contra-camber," whereby the plasma-induced momentum modified the effective aerodynamic curvature experienced by the blade. This strategy increased the peak blade lift by approximately 11% while producing a measurable increase in overall rotor thrust and simultaneously reducing the recirculation region on the suction surface. These results demonstrated that plasma actuation can provide aerodynamic benefits comparable to those achieved through mechanical design modifications while avoiding increases in rotational speed and the associated energy consumption.

The successful application of plasma actuators to cycloidal rotors encouraged their implementation in axial turbomachinery, where flow instabilities and tip leakage vortices represent major sources of aerodynamic loss. Khoshnejad et al. [99] investigated the influence of plasma-induced force orientation on the aerodynamic stability of a low-speed axial compressor rotor. Their numerical simulations revealed that actuator inclination plays a critical role in controlling the development of tip leakage vortices and delaying the onset of rotating stall. Among the investigated configurations, a negative inclination of 30° produced the most favorable aerodynamic response, increasing the compressor stability margin by approximately 8% while reducing total pressure losses near the blade tip by almost 30%. These improvements were attributed to the ability of plasma forcing to suppress backflow and weaken the leakage vortex before it developed into large-scale flow blockage, illustrating the effectiveness of DBD actuators for enhancing compressor operability.

The application of plasma actuation to turbomachinery has also been extended to aeroelastic problems involving periodically oscillating blade cascades. De Giorgi et al. [97] demonstrated that alternating-current DBD actuators can actively manipulate the unsteady aerodynamic loads responsible for flutter development in compressor cascades. Rather than focusing solely on mean flow control, their investigation emphasized the synchronization between plasma forcing and blade oscillation. Appropriate phase differences between actuators located on the pressure and suction surfaces substantially reduced lift and pitching-moment oscillations while improving aerodynamic damping. These findings highlight the versatility of plasma actuation, showing that the same phenomenological formulation originally developed for steady boundary-layer control can also be employed to regulate highly dynamic fluid–structure interactions encountered in turbomachinery.

Beyond aerodynamic performance enhancement, the Shyy model has become an important computational tool for aerothermal applications, particularly those involving film cooling technologies employed in gas turbines. Because cooling effectiveness strongly depends on coolant attachment and mixing within the boundary layer, plasma-induced momentum offers an attractive mechanism for manipulating the flow without modifying the blade geometry. Consequently, numerous numerical investigations have explored different actuator configurations, cooling-hole geometries, and operating conditions using the Shyy body-force formulation.

Li et al. [100] investigated the implementation of saw-tooth plasma actuators positioned downstream of cooling holes on turbine blades. Their large-eddy simulations demonstrated that plasma forcing significantly reduced coolant jet lift-off by weakening the counter-rotating vortex pair responsible for coolant dispersion. As a result, the cooling film remained attached to the blade surface over a longer downstream distance, increasing local cooling effectiveness by more than 20%. The study further revealed that plasma actuation reduced the intermittency of coherent vortical structures, promoting a more homogeneous coolant distribution and improving thermal protection of the blade surface.

Similar conclusions were obtained by Li et al. [101], who evaluated two different sawtooth actuator arrangements on a flat-plate film cooling configuration. Their investigation highlighted the importance of actuator geometry in determining plasma effectiveness. When the actuator tips were aligned with the center of the cooling hole, plasma forcing generated favorable anti-counter-rotating vortex pairs that expanded the coolant laterally while simultaneously forcing it toward the wall. Under these conditions, the average cooling effectiveness increased by more than 65% compared with the baseline configuration. Conversely, an unfavorable actuator orientation strengthened the natural vortical structures, increasing coolant jet lift-off and reducing thermal protection. These results demonstrated that plasma actuation effectiveness depends not only on forcing intensity but also on the interaction between actuator geometry and the inherent flow topology.

The influence of plasma forcing on film cooling has also been investigated under different cooling-hole geometries and operating conditions. Sun et al. [102] analyzed several hole configurations combined with different blowing ratios and plasma voltages. Their numerical results confirmed that the interaction between geometric optimization and plasma actuation can substantially improve thermal performance. Among the evaluated configurations, laidback fan-shaped holes combined with moderate plasma voltages produced the highest cooling effectiveness by promoting favorable anti-vortex structures while minimizing coolant mixing with the mainstream flow. Excessively high plasma voltages, however, generated local flow rebound effects that reduced cooling performance, indicating that the aerodynamic benefits of plasma forcing are not necessarily proportional to actuation intensity.

Taken together, these investigations demonstrate that the application of the Shyy phenomenological model has progressively evolved from conventional external aerodynamics toward increasingly multidisciplinary engineering problems involving rotating machinery, aeroelasticity, and thermal management. Although the governing physical phenomena differ considerably among these applications, a common mechanism underlies their success: plasma-induced momentum modifies the near-wall flow, suppresses unfavorable vortical structures, improves flow attachment, and enhances transport processes. Consequently, the Shyy formulation has established itself as a versatile computational framework capable of supporting the design and optimization of plasma-assisted technologies across a broad spectrum of turbomachinery and aerothermal systems.

Table 1 summarizes the studies that have employed Shyy's plasma body force model. For each reference, the table provides key information, including the formulation type (whether 1D, 2D, or 3D), the simulation dimensionality, the software used, and the numerical method implemented. This overview allows for a straightforward comparison of how the model has been applied across different computational frameworks and highlights the diversity of approaches in the literature.

Table 1. Summary of studies employing Shyy's plasma body force model, including formulation type (dimensionality), simulation dimensionality, software used and numerical method.

Shyy's Model				
Reference	**Form**	**1D, 2D or 3D**	**Software**	**Solution Method**
[91]	Adimensional	2D	Ansys Fluent	FEM
[98]	Dimensional	2D	Ansys Fluent	FEM
[92]	Adimensional	3D	Ansys Fluent	FVM
[97]	Adimensional	2D	Ansys Fluent	FEM
[94]	Dimensional	2D	DNS	FVM
[96]	Dimensional	3D	OpenFOAM	—
[93]	Dimensional	2D	OpenFOAM	FVM
[100]	Dimensional	2D & 3D	Ansys Fluent	FVM
[102]	Dimensional	2D	Ansys Fluent	—
[101]	Dimensional	3D	Ansys Fluent	FEM
[99]	Dimensional	3D	Ansys Fluent	FVM
[95]	Dimensional	3D	Star-CCM+	FVM
[68]	Dimensional	2D	DNS	FVM

3.2. Suzen–Huang Models

Development of the Suzen–Huang model.

The continuous advancement of dielectric barrier discharge (DBD) plasma actuators has motivated the development of increasingly sophisticated numerical models capable of representing the electrohydrodynamic (EHD) interaction between the plasma discharge and the surrounding airflow. Unlike simplified body-force approaches, the phenomenological model introduced by Suzen and Huang [71] explicitly considers the electrostatic nature of the discharge by coupling the flow solver with additional governing equations for the electric potential and charge density. This formulation provides a more physically representative description of the plasma region while maintaining a computational cost significantly lower than that required by fully coupled plasma kinetic models. Consequently, the Suzen–Huang model has become one of the most widely adopted numerical frameworks for investigating DBD plasma actuators in aerodynamic flow-control applications.

The original formulation proposed by Suzen et al. [71] represented a major milestone in plasma actuator modeling by introducing a split-potential approach in which the electric field and net charge density are computed independently before evaluating the resulting electrohydrodynamic body force. Assuming the plasma to behave as a weakly ionized gas under quasi-electrostatic conditions, the model solves Poisson's equation for the electric potential while representing the charge density through a Gaussian distribution derived from experimental observations. The resulting body force is subsequently incorporated into the Navier–Stokes equations as a momentum source term. Validation against quiescent-flow experiments demonstrated that the model successfully reproduced the characteristic wall jet generated by DBD actuators, while simulations performed on a low-pressure turbine blade confirmed its ability to delay flow separation and reduce aerodynamic losses. These results established the Suzen–Huang formulation as one of the first practical numerical tools capable of linking plasma-induced forcing with engineering-scale aerodynamic simulations.

Following its introduction, considerable research efforts focused on improving the physical realism of the original formulation while preserving its numerical efficiency. One of the earliest contributions was presented by Abdollahzadeh et al. [103], who proposed a modified split-potential formulation aimed at eliminating the empirical adjustments commonly required in previous implementations. Their approach significantly improved the prediction of plasma-induced thrust over a wide range of operating voltages while maintaining excellent agreement with available experimental measurements. An important contribution of this work was the extension of the model to high-altitude operating conditions, demonstrating that variations in atmospheric pressure and temperature substantially modify both the effective plasma length and the generated electrohydrodynamic force. These findings emphasized the importance of considering environmental conditions when designing plasma-based flow-control systems for aerospace applications.

Further improvements were introduced by Omidi and Mazaheri [104], who addressed several limitations associated with estimating plasma length, Debye length, and maximum charge density. Instead of relying on extensive experimental calibration, the authors proposed analytical relationships for estimating these parameters directly from the applied electrical conditions. Their improved formulation reduced prediction errors for plasma-induced thrust to less than 5% while accurately reproducing experimentally observed charge distributions over a broad range of operating frequencies. By incorporating more realistic electrostatic boundary conditions, the modified model substantially reduced its dependence on empirical fitting parameters without increasing numerical complexity, thereby improving its applicability to different actuator geometries and operating conditions. Collectively, these studies illustrate the progressive maturation of the Suzen–Huang model from its original electrostatic formulation toward a more robust and versatile computational framework. Although subsequent developments introduced refinements in charge-density estimation, plasma-length prediction, and environmental adaptability, the fundamental structure proposed by Suzen et al. [71] has remained largely unchanged. As a result, most contemporary implementations continue to adopt the original governing equations while incorporating localized improvements that enhance predictive capability without sacrificing computational efficiency. This balance between physical fidelity and numerical practicality largely explains why the Suzen–Huang formulation remains one of the reference phenomenological models for DBD plasma actuator simulations.

Validation and Numerical Improvements of the Suzen–Huang Model.

Following the introduction of the Suzen–Huang phenomenological formulation, considerable research efforts focused on evaluating its predictive capability and identifying opportunities for improving its physical representation of dielectric barrier discharge (DBD) plasma actuators. Rather than proposing entirely new formulations, most subsequent investigations sought to validate the model against experimental measurements, compare its performance with alternative numerical approaches, and refine specific aspects of the electrohydrodynamic force distribution. These studies collectively established the strengths and limitations of the model while providing important guidelines for its implementation in computational fluid dynamics simulations.

One of the earliest comprehensive validation studies was presented by Maden et al. [84], who combined particle image velocimetry (PIV) measurements with Reynolds-averaged Navier–Stokes simulations to evaluate two different approaches for representing plasma-induced body forces. Besides the conventional Suzen–Huang formulation, the authors proposed a velocity-based model derived directly from experimentally measured flow fields. Both approaches successfully reproduced the characteristic wall jet generated by DBD actuators and captured the pressure recovery obtained in a continuously diverging diffuser. However, the experimentally derived body-force model exhibited superior agreement with the measured velocity distribution, suggesting that inverse approaches based on PIV data may provide improved spatial accuracy while preserving computational efficiency. Their work demonstrated that experimental information can effectively complement phenomenological formulations, particularly for complex flow configurations where accurate body-force distributions are required.

Additional insight into the predictive capability of the Suzen–Huang model was obtained through direct numerical simulations. Brauner et al. [105] performed a detailed comparison between the phenomenological formulation and experimentally reconstructed forcing terms obtained from PIV measurements. Their investigation confirmed that the Suzen–Huang model accurately reproduces the temporal evolution of the initial plasma-induced vortex, validating its capability to capture the dominant macroscopic flow structures generated by DBD actuators. Nevertheless, the study also identified important physical limitations. In particular, the wall-normal component of the electrohydrodynamic force was shown to play a fundamental role in accurately reproducing the induced flow field, whereas neglecting pressure gradients—an assumption frequently adopted in simplified inverse Navier–Stokes approaches—introduced noticeable discrepancies because these gradients were found to be of the same order of magnitude as the plasma body force itself. These findings highlighted that although the phenomenological model captures the overall actuator behavior remarkably well, careful representation of all force components remains essential for high-fidelity simulations.

Several researchers subsequently investigated possible improvements to the numerical implementation of the model. Pescini et al. [106] compared three different methodologies for estimating the plasma-induced force, including the original Dual Potential Model (DPM), a simplified Single Potential Model (SPM), and an experimentally based Velocity Information Based Model (VIBM). Their comparison demonstrated that the DPM consistently provided the closest agreement with experimental measurements for both induced velocity fields and wall-jet development, whereas simplified algebraic formulations required empirical calibration to achieve acceptable accuracy. The study further demonstrated that the Suzen–Huang framework is capable of reproducing the downstream decay of the induced wall jet, an aspect that had remained difficult to predict in previous microscale actuator simulations.

Transient flow validation represented another important stage in the evolution of the model. Aono et al. [107] investigated burst-modulated plasma actuation under quiescent conditions by coupling a time-dependent implementation of the Suzen–Huang formulation with experimental schlieren and PIV measurements. Their simulations successfully reproduced both the mean wall-jet velocity and the coherent vortex structures generated during burst operation while accurately capturing the temporal fluctuations associated with different modulation frequencies. The results demonstrated that the phenomenological formulation remains valid even under highly unsteady operating conditions, extending its applicability beyond the steady-state assumptions adopted in many earlier investigations.

Further refinement of the electrohydrodynamic representation was achieved through studies focusing on specific physical mechanisms governing plasma-induced momentum transfer. Ibrahim and Skote [79] investigated the interaction between adjacent plasma actuators operating within confined channel flows. Their modified Suzen–Huang implementation successfully reproduced the experimentally observed velocity distributions for relatively large channel heights but also revealed important discrepancies under highly confined conditions. The study suggested that microscopic plasma phenomena and charge-interaction mechanisms, which are not explicitly represented in phenomenological formulations, become increasingly significant as confinement intensifies. Consequently, the authors emphasized that, although the Suzen–Huang model provides reliable predictions for most engineering-scale applications, additional physical modeling may be required for microscale and strongly confined flow configurations.

Complementary investigations also explored the influence of actuator geometry and electrical operating parameters on plasma performance. Seth et al. [73] analyzed the effects of dielectric thickness, electrode spacing, excitation frequency, and voltage waveform on the electrohydrodynamic force generated by DBD actuators using a transient implementation of the Suzen–Huang formulation. Their numerical results showed that relatively small geometric modifications can significantly alter both the induced ionic wind and the resulting body force, while square-wave excitation consistently generated stronger plasma-induced velocities than sinusoidal or triangular waveforms. These findings demonstrated that actuator performance depends not only on the numerical formulation itself but also on the electrical and geometric characteristics adopted during the design process.

Taken together, these validation and refinement studies significantly strengthened the credibility of the Suzen–Huang phenomenological model. Despite differences in numerical implementation, experimental configuration, and validation methodology, a consistent conclusion emerges throughout the literature: the model accurately reproduces the dominant macroscopic effects of DBD plasma actuation while maintaining a computational cost compatible with engineering-scale simulations. At the same time, these investigations clearly identify the principal sources of uncertainty, including pressure-gradient effects, wall-normal force components, actuator confinement, and parameter calibration. Consequently, the Suzen–Huang formulation has evolved into one of the most thoroughly validated phenomenological models available, providing a reliable foundation for the broad range of aerodynamic, turbomachinery, and aerothermal applications discussed in the following sections.

Table 2 summarizes the studies that have adopted the Suzen–Huang plasma body force model. For each work, the table presents the formulation type (distinguishing between 1D, 2D, and 3D approaches), the simulation dimensionality, the software employed, and the numerical method used. This compilation provides a clear comparative view of the model's implementation across various computational environments and illustrates the range of numerical strategies reported in the literature.

Table 2. Summary of studies employing Suzen–Huang plasma body force model, including formulation type (dimensionality), simulation dimensionality, software used and numerical method.

Suzen's Model				
Reference	**Form**	**1D, 2D or 3D**	**Software**	**Solution Method**
[84]	Dimensional	2D	OpenFOAM	FVM
[108]	Adimensional	2D	—	FVM
[105]	Adimensional	2D	—	FEM
[71]	Adimensional	2D	GHOST	FVM
[52,73,103,109]	Adimensional	2D	Ansys Fluent	FVM
[110]	Adimensional	2D	Incompact3d	—
[79]	Dimensional	2D & 3D	Ansys Fluent	FVM
[106]	Adimensional	2D	CONSDI	FVM
[104]	Dimensional	2D	Ansys Fluent	—
[111]	Adimensional	2D & 3D	Ansys Fluent	FVM
[112]	Adimensional	3D	Ansys Fluent	FEM
[113]	Dimensional	2D	PROPID-53	FEM
[114]	Dimensional	2D	Ansys Fluent	—

3.3. Dörr and Kloker Model

Development of the empirical model.

Although most phenomenological formulations estimate the electrohydrodynamic body force from simplified electrostatic equations, an alternative modeling strategy has emerged in which the force distribution is reconstructed directly from experimentally measured flow fields. This empirical approach seeks to reproduce the macroscopic effects of dielectric barrier discharge (DBD) plasma actuators without explicitly solving the electric potential or charge-density equations, thereby reducing model complexity while preserving the experimentally observed characteristics of the induced wall jet. Among these approaches, the empirical model proposed by Maden et al. [84] and subsequently extended by Dörr and Kloker [83,115] represents one of the most significant alternatives to conventional phenomenological formulations.

The work of Maden et al. [84] introduced a data-driven methodology in which the spatial distribution of the electrohydrodynamic body force was reconstructed from particle image velocimetry (PIV) measurements obtained under quiescent conditions. Rather than relying on simplified assumptions regarding the electric field or charge density, the proposed formulation employed analytical functions fitted directly to experimentally measured velocity fields to determine the body-force distribution. Comparative analyses performed against the Shyy and Suzen models demonstrated that the empirical formulation reproduced the wall-jet velocity profile with significantly higher spatial accuracy, particularly within the plasma region where conventional phenomenological models either underestimated or excessively concentrated the applied force. These results demonstrated that experimental reconstruction techniques could substantially improve the representation of plasma-induced momentum transfer while remaining compatible with conventional computational fluid dynamics solvers.

The growing interest in experimentally derived body-force distributions motivated further investigations into the physical assumptions underlying empirical plasma models. Dörr and Kloker [83] conducted a comprehensive numerical assessment of force-reconstruction methodologies by comparing different inverse formulations based on velocity-field information. Their analysis demonstrated that pressure gradients cannot be neglected when reconstructing the electrohydrodynamic force in the presence of a background flow, since their contribution becomes comparable to that of the plasma-induced forcing itself. Furthermore, although the wall-normal component of the force exhibited only a limited influence on the global flow development, neglecting this contribution affected the accuracy of the reconstructed force field under certain operating conditions. These findings provided an important physical interpretation of the empirical approach, clarifying both its capabilities and its inherent limitations.

Unlike electrostatic formulations such as the Shyy and Suzen–Huang models, the empirical methodology developed by Maden and later refined by Dörr and Kloker is fundamentally driven by experimental observations rather than by simplified plasma physics. Consequently, its predictive capability depends strongly on the quality and representativeness of the experimental database used during model construction. Nevertheless, this characteristic also constitutes one of its principal advantages, since the reconstructed body-force distribution naturally incorporates physical effects that are often neglected by simplified electrostatic formulations. As a result, the Dörr–Kloker empirical model has become an attractive alternative for applications requiring highly accurate representations of the induced wall jet while avoiding the computational complexity associated with detailed plasma-discharge simulations.

Validation and engineering applications of the Dörr–Kloker empirical model.

Following the development of the empirical body-force formulation, subsequent investigations focused on evaluating its capability to reproduce plasma-induced flow control under increasingly realistic aerodynamic conditions. Unlike the original studies conducted in quiescent environments, these investigations assessed the model in the presence of external flows, pressure gradients, and transitional boundary layers, thereby establishing its applicability to practical engineering problems. Collectively, these studies demonstrated that experimentally reconstructed body-force distributions provide a reliable alternative to conventional electrostatic formulations while simultaneously revealing the limitations associated with data-driven approaches.

One of the first engineering applications of the Dörr–Kloker methodology addressed the control of laminar-to-turbulent transition in boundary-layer flows. Dörr and Kloker [115] incorporated the experimentally reconstructed body-force distribution into direct numerical simulations of a flat-plate boundary layer subjected to free-stream disturbances. Their results demonstrated that DBD plasma actuation effectively delayed transition by attenuating the growth of instability waves responsible for turbulence onset. The plasma-induced wall jet redistributed momentum within the near-wall region, reducing disturbance amplification and extending the laminar flow regime over a significant downstream distance. Beyond confirming the effectiveness of plasma actuation, this work demonstrated that empirical body-force reconstruction could successfully reproduce highly sensitive instability mechanisms without requiring explicit electrostatic calculations.

The applicability of experimentally reconstructed force fields was subsequently extended to more complex aerodynamic configurations. Wang et al. [116] investigated plasma-based active flow control under external aerodynamic conditions representative of practical engineering applications. Their numerical simulations confirmed that body-force distributions derived from experimental measurements accurately predicted the interaction between plasma forcing and the surrounding flow, reproducing the principal characteristics of boundary-layer acceleration and separation control observed experimentally. The study emphasized that empirical formulations naturally preserve the spatial distribution of the electrohydrodynamic force generated by the actuator, allowing realistic simulations even when detailed plasma physics remain unresolved. These findings reinforced the potential of data-driven plasma models for engineering-oriented computational fluid dynamics analyses, particularly in situations where experimental information is available for model calibration.

Although empirical formulations demonstrated excellent agreement with experimental observations, their predictive capability remains inherently linked to the quality and representativeness of the experimental database from which the body-force distribution is reconstructed. Consequently, recent research has focused on evaluating the performance of empirical and phenomenological formulations within a common computational framework in order to establish their respective advantages and limitations.

An important contribution in this direction was presented by Bernal-Orozco et al. [69], who performed one of the first systematic comparisons between the three phenomenological approaches most frequently employed for dielectric barrier discharge plasma actuators: the Shyy model, the Suzen–Huang formulation, and the empirical Dörr–Kloker methodology. Using identical numerical conditions, the authors evaluated the predictive capability, computational efficiency, and implementation complexity of each approach. Their results showed that all three models successfully reproduced the principal macroscopic characteristics of plasma-induced flow control, including the generation of the wall jet and the resulting momentum transfer to the surrounding fluid. However, important differences emerged regarding their physical representation and numerical requirements. The Shyy formulation provided the simplest implementation and the lowest computational cost, making it particularly attractive for large-scale engineering simulations. In contrast, the

Suzen–Huang model offered a more physically representative description of the plasma discharge through the solution of additional electrostatic equations, albeit with increased computational complexity. The empirical Dörr–Kloker approach exhibited the closest agreement with experimentally reconstructed velocity fields because the body-force distribution was directly derived from experimental measurements. Nevertheless, its applicability remained strongly dependent on the availability of high-quality experimental data, limiting its predictive capability for configurations lacking prior measurements.

The comparative analysis performed by Bernal-Orozco et al. [69] clearly illustrates that no single phenomenological model is universally superior for every application. Instead, the selection of an appropriate formulation depends on the specific objectives of the numerical investigation. When computational efficiency and ease of implementation are prioritized, simplified body-force models such as Shyy remain highly competitive. Conversely, simulations requiring a more detailed representation of the electrostatic field benefit from the Suzen–Huang formulation, whereas empirical approaches provide the highest level of agreement with experimental observations whenever reliable calibration data are available. This comparative perspective represents an important milestone in the evolution of plasma actuator modeling because it shifts the discussion from identifying the “best” model toward selecting the formulation most appropriate for a given engineering application.

Overall, the available literature demonstrates that the Dörr–Kloker empirical model constitutes a valuable complement to conventional phenomenological formulations rather than a direct replacement. By combining experimentally reconstructed body-force distributions with computational fluid dynamics simulations, the model provides an effective compromise between physical realism and numerical efficiency for applications where detailed experimental information is available. At the same time, the comparative studies published in recent years have clarified the relative strengths and limitations of empirical and electrostatic approaches, providing researchers with a more comprehensive framework for selecting the most suitable plasma model according to the complexity, computational resources, and objectives of each investigation.

Table 3 summarizes the studies that have utilized Dörr’s plasma body force model. For each reference, the table details the formulation type (categorized by dimensionality, i.e., 1D, 2D, or 3D), the simulation dimensionality, the software employed, and the numerical method implemented. This overview facilitates a direct comparison of how the model has been applied across different computational setups and underscores the variety of numerical approaches found in the existing literature.

Table 3. Summary of studies employing Dörr’s plasma body force model, including formulation type (dimensionality), simulation dimensionality, software used and numerical method.

Dörr’s Model				
Reference	**Form**	**1D, 2D or 3D**	**Software**	**Solution Method**
[115]	Adimensional	3D	NS3D (DNS)	FDM
[84]	Dimensional	2D	OpenFOAM	FVM
[116]	Adimensional	3D	DNS	NPSE-FDM
[83]	Adimensional	2D	NS3D	FEM
[69]	Dimensional	3D	OpenFOAM	FVM

3.4. Other Models

Physically based plasma-fluid models.

The development of physically based plasma-fluid models represented one of the first approaches to describe the complex interaction between dielectric barrier discharge (DBD) plasma actuators and the surrounding flow. Unlike simplified phenomenological formulations, these models attempt to directly resolve the fundamental mechanisms governing plasma generation, charge transport, electric field distribution, and momentum transfer from charged species to the neutral gas. Consequently, they provide a more comprehensive description of the electrohydrodynamic (EHD) forces generated by plasma actuators, although at the expense of significantly higher computational requirements due to the multiple spatial and temporal scales involved.

Early efforts focused on establishing self-consistent plasma-fluid formulations capable of coupling plasma dynamics with fluid motion. Jayaraman et al. [117] developed a two-fluid numerical framework for atmospheric-pressure non-thermal plasma discharges, where the plasma phase and the neutral gas were coupled through electric forces and pressure contributions. The model solved the continuity, momentum, and energy equations for charged species together with the Poisson equation for the electric field, while the induced flow was described through the incompressible Navier–Stokes equations. This approach demonstrated that the plasma-generated body force could be obtained directly from charge distributions rather than through empirical assumptions, providing a more physically consistent prediction of the ionic wind generated by DBD actuators. However, the authors also highlighted the increased computational complexity associated with resolving plasma transport phenomena over significantly smaller time scales than those governing aerodynamic flows.

Subsequent studies improved these formulations by incorporating more detailed descriptions of charge transport and electric field evolution. Singh and Roy [118] proposed a self-consistent multiphysics model based on the drift-diffusion approximation for electrons and ions coupled with the Poisson equation. Using a finite element formulation, they analyzed the influence of voltage amplitude and excitation frequency on the electrodynamic force generated by asymmetric DBD actuators. Their results demonstrated that the induced force increases strongly with the applied voltage, following an approximately fourth-power relationship, and that the resulting velocity profiles were comparable with those obtained from simplified force approximations. This study established a direct relationship between electrical operating parameters and aerodynamic performance, although the computational cost limited the application of the model to relatively small computational domains.

Further advances were introduced by Jayaraman et al. [63], who investigated the physical mechanisms governing asymmetric DBD actuators through a coupled electric field, plasma transport, and momentum formulation. Their model solved the Poisson equation, charged-particle transport equations, and fluid momentum equations using a finite-volume approach. The transient simulations allowed the evolution of force generation during the voltage cycle to be analyzed, revealing the dependence of the induced momentum on electrode geometry, dielectric properties, and voltage waveform. The study showed that the asymmetry of charge accumulation during the discharge cycle plays a fundamental role in producing a net directional force, providing important insights into the optimization of actuator configurations.

The need for accurate representation of transient plasma phenomena motivated the development of more advanced numerical strategies. Papageorgiou et al. [119] developed a three-dimensional model for atmospheric-pressure gaseous discharges including photoionization effects through Helmholtz equations. Their work compared fully three-dimensional simulations with axisymmetric two-dimensional approaches, demonstrating good agreement in electron density and current distributions while emphasizing the considerable computational cost associated with three-dimensional plasma simulations. The authors showed that although three-dimensional models are necessary for capturing complex instabilities and asymmetric discharge structures, two-dimensional formulations remain essential for practical engineering applications where computational efficiency is a priority.

The implementation of plasma-fluid models into open-source computational frameworks further expanded their accessibility for flow-control studies. Abdollahzadeh et al. [120] implemented a classical plasma-fluid formulation within OpenFOAM, coupling charged-species transport equations, the Poisson equation, and fluid dynamics. Their approach incorporated numerical strategies such as operator splitting and super-time-stepping methods to improve stability and computational efficiency when solving highly transient plasma phenomena. The results demonstrated that the predicted current density and EHD force distributions were strongly affected by the applied voltage waveform, confirming the importance of accurately capturing the temporal evolution of charge accumulation and electric-field formation.

More recently, plasma-fluid models have been extended to analyze specific discharge characteristics and waveform effects. Singh and Roy [121] investigated the spatial and temporal evolution of charge separation in asymmetric DBD actuators, demonstrating that the accumulation of surface charges on the dielectric generates a non-uniform electric field responsible for the directional electrohydrodynamic force. Similarly, Chen et al. [122] analyzed pulsed-DC DBD actuators with fast-rise-slow-decay voltage waveforms using a transient fluid model. Their results revealed that the discharge evolution can be divided into distinct stages, where the rapid voltage rise primarily generates the plasma channel, while the decay stage contributes predominantly to thrust production. These studies highlighted the importance of waveform optimization as a mechanism to improve energy conversion efficiency in plasma-based flow-control systems.

Despite their high predictive capability, physically based plasma-fluid models remain computationally demanding due to the disparity between plasma and aerodynamic time scales, the requirement of fine spatial discretization near electrodes, and the need to solve strongly coupled nonlinear equations. Therefore, their application has been mainly limited to fundamental investigations, actuator characterization, and the generation of physically meaningful databases for reduced-order models. Nevertheless, these approaches provide the most complete description of DBD actuator operation and constitute the reference framework for the development and validation of simplified models intended for large-scale engineering applications.

Phenomenological body-force models.

Although physically based plasma-fluid models provide a detailed description of the discharge process and the resulting electrohydrodynamic (EHD) forces, their computational cost limits their direct application to large-scale engineering problems. To overcome this limitation, phenomenological body-force models have been developed as an alternative approach, where the effect of the plasma actuator is represented as an equivalent momentum source term incorporated into the Navier–Stokes equations. These formulations neglect the detailed plasma chemistry and charge transport mechanisms, but they provide a practical balance between computational efficiency and predictive capability, enabling the simulation of plasma actuators in complex aerodynamic configurations.

One of the first approaches toward experimentally derived body-force modeling was reported by Kotsonis and Ghaemi [123], who developed a methodology to estimate the spatial distribution of the force generated by DBD actuators from time-resolved particle image velocimetry (PIV) measurements. By applying the momentum conservation equation to experimentally obtained velocity fields, the authors reconstructed the plasma-induced force distribution without explicitly resolving the plasma discharge. The proposed approach was validated for both continuous and pulsed actuation modes, showing good agreement between numerical predictions and experimental measurements. However, the authors also identified that experimentally derived force distributions provide limited predictive capability because new measurements are required when operating conditions or actuator geometries are modified.

A complementary experimental methodology was proposed by Kotsonis et al. [124], who investigated the spatial distribution of the body force generated by DBD actuators through high-speed PIV measurements. By combining velocity-field measurements with the Navier–Stokes equations, the authors obtained the force vector distribution acting on the flow and compared the results with direct thrust measurements using a high-sensitivity load cell. The good agreement between both approaches demonstrated the feasibility of using experimentally reconstructed force fields as a validation tool for numerical models. Their results also revealed the strong influence of excitation voltage and frequency on the size and magnitude of the induced flow region, highlighting the importance of actuator operating parameters in determining the aerodynamic response.

To reduce the dependency on experimental calibration, semi-empirical formulations were later developed by relating the induced force to measurable electrical and geometrical parameters. Singh and Roy [118] introduced a functional approximation for the electrodynamic force generated by DBD actuators, derived from a self-consistent plasma model and expressed as a function of voltage amplitude and actuator characteristics. Their formulation provided a simplified representation of the plasma effect that could be directly integrated into fluid solvers, while maintaining the relationship between electrical excitation and induced momentum. Similarly, Yoon and Han [125] proposed an improved thrust model based on electrostatic pressure generation, incorporating environmental conditions, dielectric properties, electrode dimensions, voltage amplitude, and excitation frequency. The model was validated against a large experimental dataset and achieved acceptable accuracy, demonstrating that simplified formulations can reproduce the main trends of actuator performance without resolving the complete plasma discharge process.

Phenomenological models have also been widely adopted for aerodynamic flow-control studies due to their straightforward implementation in commercial and open-source CFD platforms. Szulga et al. [126] developed an empirical body-force representation of a DBD actuator based on velocity measurements and applied it to investigate boundary-layer transition control over an airfoil. The model successfully reproduced the stabilizing effect of the actuator when positioned near the transition region, although discrepancies between numerical and experimental results indicated the limitations of simplified forcing approaches in capturing localized velocity overshoots and complex interactions with instability waves. Similarly, Liu et al. [127] incorporated a quasi-steady body-force model into Reynolds-averaged Navier–Stokes simulations to evaluate the influence of SDBD actuators on Tollmien–Schlichting wave attenuation and drag reduction. Their results demonstrated that actuator position and forcing intensity strongly affect transition delay, while also emphasizing the challenge of achieving positive energy efficiency due to the relatively high electrical consumption of plasma actuators.

The simplicity of phenomenological formulations has enabled their application beyond aerodynamic flow control. Chen et al. [128] employed a simplified representation of nanosecond DBD thermal effects to analyze flap-flow control, demonstrating that pulse width and energy density significantly influence lift enhancement and separation delay. In another application, Sumanik et al. [129] modeled a DBD actuator as a tangential velocity boundary condition to investigate aerodynamic control of a sounding rocket. Their approach demonstrated that plasma-induced momentum addition could generate measurable control moments without mechanical moving surfaces, although the simplified boundary condition does not capture the detailed physics of plasma-flow interaction.

To further improve computational efficiency, hybrid formulations combining analytical solutions with empirical information have been proposed. Amanifard et al. [130] introduced a reduced-order model based on the similarity solution of a laminar wall jet, where the plasma actuator effect was represented through an imposed velocity profile rather than a distributed body force. This approach significantly reduced computational requirements while maintaining reasonable agreement with experimental velocity distributions, making it suitable for parametric studies and optimization procedures. However, the authors noted that the simplified representation may not accurately capture local discharge effects or complex transient phenomena.

Overall, phenomenological body-force models have become the most widely used approach for engineering-scale simulations of plasma actuators due to their reduced computational cost and compatibility with conventional CFD frameworks. Their main advantage lies in enabling the integration of plasma effects into complex geometries, turbulent flows, and multiphysics applications that would be computationally prohibitive using fully coupled plasma-fluid models. Nevertheless, their predictive capability remains strongly dependent on calibration procedures, actuator configuration, and operating conditions. Consequently, current research trends are increasingly focused on developing hybrid strategies that combine the physical consistency of plasma-fluid formulations with the efficiency required for practical engineering applications.

Reduced-order and hybrid models.

The limitations associated with both fully coupled plasma-fluid models and purely empirical body-force formulations have motivated the development of reduced-order and hybrid modeling strategies. These approaches aim to preserve the dominant physical mechanisms responsible for plasma-induced momentum transfer while reducing computational requirements. By combining analytical descriptions, experimental correlations, electrical models, and simplified plasma representations, hybrid models provide an intermediate level of fidelity that is particularly attractive for optimization procedures, multiparametric studies, and engineering-scale simulations.

One of the main challenges in plasma actuator modeling is the representation of the complex relationship between electrical excitation and aerodynamic performance. Erfani et al. [131] addressed this problem by combining experimental characterization with numerical optimization techniques to determine an optimal DBD actuator configuration. Instead of resolving the complete plasma discharge physics, the authors developed a response surface methodology (RSM) based on experimental velocity measurements, relating induced flow velocity to design parameters such as voltage, frequency, and electrode geometry. The optimization process, performed using a D-optimal design strategy, significantly reduced the number of required experiments while identifying configurations capable of increasing induced velocity compared with conventional designs. This approach demonstrated the potential of reduced-order models as efficient tools for actuator design optimization, although their applicability remains limited to the parameter space covered during model development.

Another important direction in hybrid modeling involves the integration of simplified electrical representations with fluid simulations. Zhang et al. [132] developed a coupled magnetohydrodynamic (MHD) and equivalent RLC circuit model to investigate energy deposition, heat transfer, and efficiency in plasma actuators. The electrical model reproduced the discharge behavior, while the MHD formulation provided the coupling between plasma properties and fluid motion. The results showed that energy losses are strongly influenced by the discharge evolution, with the sheath region accounting for a significant fraction of the dissipated energy. This work highlighted that simplified electrical models can provide valuable information about actuator efficiency while avoiding the computational cost of resolving the complete plasma chemistry and charge transport mechanisms.

Reduced-order formulations have also been implemented through user-defined functions and semi-empirical force models within commercial CFD environments. Moayedi and Amanifard [133] investigated the enhancement of natural convection heat transfer using multiple DBD actuators by introducing a semi-empirical plasma-induced body-force model into ANSYS Fluent. Their approach represented the electrical force as a function of applied voltage and actuator parameters, allowing the influence of actuator number and arrangement on thermal performance to be evaluated. The results demonstrated that multiple actuators can significantly enhance heat transfer, while also revealing the existence of an optimal number of actuators when energy consumption is considered. This study illustrates the advantage of reduced-order approaches for exploring design variables in multiphysics systems where fully resolved plasma simulations would be impractical.

Hybrid approaches have also been extended to plasma-assisted combustion, where the interaction between plasma chemistry, fluid dynamics, and combustion processes introduces additional modeling challenges. Mardani and Khanehzar [134] evaluated the effect of nanosecond repetitive DBD plasma on MILD combustion using a simplified plasma representation incorporated into a reacting-flow model. Rather than explicitly resolving plasma generation, the authors introduced plasma effects through modified boundary conditions involving reactive species and thermal contributions. Their results showed that plasma actuation enhanced flame stability, increased radical production, and extended the operational range of diluted combustion regimes. Although this approach simplified the plasma physics, it provided valuable insight into the dominant thermal and kinetic effects governing plasma-assisted combustion.

A more detailed hybrid plasma-combustion coupling was proposed by Massa and Freund [135], who developed a three-dimensional numerical framework combining simplified plasma microstreamer dynamics with combustion chemistry and turbulent flow modeling. The model incorporated plasma-induced source terms while avoiding the computational expense of resolving individual discharge events. The simulations successfully reproduced experimentally observed trends in ignition probability and flame stabilization, demonstrating that appropriately simplified plasma descriptions can capture the essential mechanisms governing plasma-assisted combustion under realistic flow conditions.

Hybrid formulations have also been developed for applications involving fluid-structure interaction (FSI) and complex flow control problems. Russo et al. [136] investigated the influence of DBD actuators on the oscillatory response of an elastic structure subjected to vortex-induced vibrations. The plasma actuator was represented through a simplified tangential velocity boundary condition characterized by actuation intensity and frequency. This reduced-order approach enabled the analysis of synchronization phenomena between plasma forcing and structural oscillations, demonstrating the potential of plasma actuators as active flow-control devices for FSI applications. However, the simplified representation inherently neglects the transient plasma dynamics responsible for the generation of the induced momentum.

The combination of analytical formulations and empirical information has also led to efficient models for rapid prediction of plasma-induced flow fields. Amanifard et al. [130] proposed a hybrid analytical-empirical model based on the similarity solution of a laminar wall jet, where the plasma-induced velocity profile was introduced as a boundary condition in CFD simulations. Compared with conventional body-force approaches, this methodology reduced computational complexity while maintaining good agreement with experimental measurements. The authors demonstrated that the approach is suitable for preliminary design and optimization studies, although the simplified treatment limits its ability to reproduce complex discharge phenomena.

Overall, reduced-order and hybrid models represent an important transition between fundamental plasma simulations and practical engineering applications. Their main contribution is the ability to incorporate relevant plasma effects into large-scale computational analyses while maintaining manageable computational costs. However, these approaches involve a compromise between physical fidelity and efficiency, since simplifications may limit their predictive capability outside the conditions used for calibration. Future developments are therefore expected to focus on adaptive hybrid frameworks that combine physically based plasma descriptions with data-driven and reduced-order techniques, enabling accurate yet computationally efficient simulations for the design and optimization of plasma-assisted systems.

Multiphysics applications of DBD plasma actuators.

The versatility of dielectric barrier discharge (DBD) plasma actuators has enabled their application in a wide range of multiphysics problems, including aerodynamic flow control, combustion enhancement, thermal management, and fluid–structure interaction. The ability of these devices to introduce momentum, modify boundary-layer characteristics, generate localized heating, and influence chemical reactions without mechanical moving components has positioned plasma actuation as an attractive alternative for advanced control systems. Consequently, numerical modeling approaches have been increasingly employed to evaluate their effectiveness in complex engineering environments.

Aerodynamic flow control.

Aerodynamic flow control remains the most extensively investigated application of DBD plasma actuators due to their capability to modify near-wall flow structures through electrohydrodynamic momentum transfer. Early studies demonstrated that plasma-induced body forces can influence boundary-layer development, separation behavior, and transition mechanisms, providing an alternative to conventional mechanical control devices.

Abdollahzadeh et al. [137] investigated the interaction between nanosecond DBD plasma-generated shock waves and transonic flow using a coupled plasma-fluid numerical model. Their results demonstrated that rapid energy deposition from the discharge generates localized pressure disturbances capable of modifying the flow characteristics around aerodynamic surfaces. The study highlighted the potential of nanosecond plasma actuators for high-speed flow manipulation while maintaining lower computational requirements compared with fully resolved plasma simulations.

The ability of plasma actuators to delay boundary-layer transition and control instabilities has also been extensively explored. Shang and Huang [138] analyzed the use of plasma actuators for controlling cross-flow instabilities over swept wings. Their simulations showed that plasma actuation reduced the amplitude of cross-flow vortices and delayed the transition to turbulence by modifying the instability growth mechanisms. Similarly, Liu et al. [127] evaluated the influence of SDBD actuators on Tollmien–Schlichting wave development and drag reduction in an airfoil configuration. Their results demonstrated that actuator position and forcing intensity strongly affect transition delay, although the energy efficiency remained limited due to the high electrical power consumption required for actuation.

Plasma actuators have also been investigated for improving aerodynamic performance in high-lift configurations. Chen et al. [128] studied the influence of nanosecond DBD operating parameters on the aerodynamic behavior of a flap-equipped airfoil. Their results indicated that pulse width and energy density significantly affect separation control, with optimized conditions producing improvements in lift generation and drag reduction. These findings demonstrate that plasma actuation can provide effective flow manipulation during critical aerodynamic conditions, such as take-off and landing, where conventional mechanical systems become less efficient.

Beyond conventional aircraft applications, plasma actuators have been explored for aerodynamic control in aerospace systems. Sumanik et al. [129] proposed a simplified DBD model to investigate the generation of aerodynamic moments on sounding rocket fins. Their results showed that plasma-induced momentum could generate measurable roll control without requiring mechanical actuators. Although the simplified boundary condition employed in the study does not fully capture plasma dynamics, it demonstrated the feasibility of using DBD actuators as lightweight and compact control devices for aerospace applications.

Plasma-assisted combustion.

In addition to aerodynamic applications, DBD plasma actuators have attracted significant attention in combustion systems due to their ability to generate reactive species, modify local temperature fields, and enhance ignition processes. Plasma-assisted combustion represents a highly coupled multiphysics problem involving plasma kinetics, chemical reactions, heat transfer, and turbulent transport.

Song et al. [139] investigated the ionization characteristics of methane-air mixtures subjected to DBD plasma discharge, focusing on the generation of reactive species and their influence on combustion enhancement. Their results demonstrated that plasma excitation promotes the formation of chemically active species, particularly under lean conditions, improving the potential for ignition and flame stabilization.

Mardani and Khanehzar [134] analyzed the effects of nanosecond repetitive DBD plasma on MILD combustion systems. By incorporating plasma-induced thermal and chemical effects into reacting-flow simulations, they demonstrated that plasma actuation enhances reaction rates, increases radical production, and extends the operational range of diluted combustion regimes. Their results emphasized that thermal, kinetic, and dynamic effects contribute simultaneously to combustion improvement, with the relative importance depending on operating conditions.

A more detailed plasma-combustion interaction was investigated by Massa and Freund [135], who developed a hybrid numerical framework to describe plasma-assisted ignition in a hydrogen jet under cross-flow conditions. The model captured the influence of plasma microstructures on energy deposition and flame initiation, reproducing experimental trends in ignition probability and absorbed power. Their results demonstrated that simplified plasma representations can successfully describe the dominant mechanisms controlling ignition while avoiding the prohibitive computational cost of resolving individual discharge events.

Experimental and numerical investigations have also explored the influence of plasma actuation on burner flow dynamics. Pescini et al. [140] characterized the effects of AC-DBD actuators on coaxial jet flows in a Bunsen burner configuration. Their results showed that plasma actuation modifies velocity fluctuations, mixing characteristics, and flame behavior through combined thermal and momentum effects. This dual influence highlights the importance of considering both fluid dynamic and chemical mechanisms when designing plasma-assisted combustion systems.

Thermal management and heat transfer enhancement.

The capability of DBD actuators to modify near-wall flow structures has also motivated their application in thermal management systems. Moayedi and Amanifard [133] investigated the enhancement of natural convection heat transfer in vertical channels using multiple plasma actuators. By introducing a semi-empirical body-force model into CFD simulations, they evaluated the effects of actuator number and arrangement on thermal performance. Their results demonstrated significant increases in the Nusselt number due to boundary-layer destabilization and enhanced fluid mixing. However, the study also revealed the existence of an optimal actuator configuration, since additional devices increase energy consumption without proportional thermal benefits.

These findings indicate that plasma actuators may provide an alternative method for active thermal control, particularly in systems where conventional cooling strategies are limited by space, weight, or mechanical complexity. Nevertheless, further investigations are required to improve energy efficiency and evaluate long-term operational reliability.

Fluid–structure interaction and advanced control applications.

The influence of plasma actuators has recently been extended to coupled fluid–structure systems, where flow modification can directly affect structural dynamics. Russo et al. [136] investigated the application of DBD actuation to control vortex-induced vibrations in a flexible structure. By modeling the actuator through a simplified tangential velocity boundary condition, they demonstrated that plasma forcing can modify vortex shedding behavior, reduce structural oscillations, and achieve synchronization between actuation frequency and structural response.

This application represents a significant expansion of plasma actuator technology beyond traditional aerodynamic control, suggesting potential applications in adaptive structures, vibration suppression, and energy harvesting systems. However, the development of accurate models capable of simultaneously capturing plasma dynamics, turbulent flow behavior, and structural deformation remains an open challenge.

Overall, the reviewed studies demonstrate that DBD plasma actuators have evolved from aerodynamic flow-control devices into multifunctional systems capable of influencing coupled physical phenomena. Despite significant advances, practical implementation remains limited by challenges related to energy efficiency, actuator durability, and accurate prediction under realistic operating conditions. Future developments will likely depend on the integration of advanced reduced-order models, experimental validation techniques, and optimization frameworks capable of designing plasma-based control systems for complex engineering applications.

Table 4 summarizes the studies that have employed other plasma body force models not covered in the previous tables. For each reference, the table provides the formulation type (distinguishing between 1D, 2D, and 3D approaches), the simulation dimensionality, the software used, and the numerical method implemented. This compilation offers a comprehensive overview of alternative modeling strategies and serves as a complement to the preceding summaries.

Table 4. Summary of studies employing other models, including formulation type (dimensionality), simulation dimensionality, software used and numerical method.

Other Models				
Reference	**Dimensional or Nondimensional**	**Domain**	**Software**	**Solution Method**
[137]	Dimensional	2D	In-house code	Coupled plasma-fluid model solving energy deposition and compressible Navier–Stokes equations
[63]	Dimensional	2D	In-house code	Plasma–fluid model including species transport and Poisson equation, solved using finite volumes
[124]	Dimensional	2D (experimental, planar velocity field)	DaVis 7.4	High-speed PIV with body-force estimation via momentum balance

Table 4. *Cont.*

Other Models				
Reference	Dimensional or Nondimensional	Domain	Software	Solution Method
[141]	Dimensional	2D	COMSOL	Transient FEM model solving Maxwell's equations with field-dependent properties
[131]	Dimensional	2D (planar PIV measurements)	MATLAB	Quasi-steady PIV + DBD, RSM turbulence modeling and numerical optimization
[138]	Dimensional	3D	In-house code	Transient CFD with phenomenological plasma model for boundary-layer control
[139]	Dimensional	1D (parallel-plate discharge)	In-house code + BOLSIG+	1D plasma model with transport, ionization and electron–particle collisions
[142]	Dimensional	2D	In-house DNS code	Direct numerical simulation of incompressible Navier–Stokes with plasma-induced body force
[134]	Dimensional	2D axisymmetric	CHEMKIN	RANS CFD with combustion; plasma modeled as thermal and species source terms
[129]	Dimensional	2D	OpenFOAM	RANS CFD with DBD modeled as a tangential velocity boundary condition
[132]	Dimensional	2D	ANSYS Fluent	Coupled CFD–plasma model with electrical circuit and RSM turbulence model
[133]	Dimensional	2D	ANSYS Fluent	Natural convection CFD with semi-empirical plasma body-force model
[135]	Dimensional	3D	In-house solver	CFD–plasma model with plasma source terms and hybrid modeling approach
[127]	Dimensional	2D	PMNS2D	Boundary-layer CFD with quasi-steady plasma force and linear stability analysis
[120]	Dimensional	2D	OpenFOAM	Coupled plasma–fluid model solving species transport, charge density and Poisson equation
[123]	Dimensional	2D (experimental + numerical)	OpenFOAM	Hybrid PIV–CFD approach with experimentally derived body force
[128]	Dimensional	2D	ANSYS Fluent 17.1	Transient RANS CFD with NS–DBD actuator modeled as a thermal perturbation
[140]	Dimensional	2D axisymmetric (experimental + numerical)	ANSYS Fluent	Hybrid experimental–numerical model with plasma treated as a thermal source
[130]	Dimensional	2D	ANSYS Fluent	Analytical–empirical model where the DBD is imposed as a wall jet
[136]	Dimensional	2D (FSI)	In-house solver	Laminar FSI simulation with DBD modeled as tangential wall slip
[119]	Dimensional	3D (compared with 2D axisymmetric)	In-house code	Transient plasma model solving Poisson equation, species transport and photoionization

Table 4. *Cont.*

Other Models				
Reference	**Dimensional or Nondimensional**	**Domain**	**Software**	**Solution Method**
[125]	Dimensional	2D	ANSYS Fluent	CFD with physics-based empirical thrust model calibrated against PIV
[117]	Dimensional	2D (asymmetric DBD model)	STREAM	Two-fluid plasma–flow model coupled through electrohydrodynamic (EHD) force
[120]	Dimensional	2D (classical DBD, atmospheric air)	OpenFOAM	Classical transient plasma–fluid model with electrohydrodynamic force
[118]	Dimensional	2D	In-house FEM	Empirical DBD force model coupled with boundary-layer flow and stability analysis
[126]	Dimensional	2D (boundary layer)	ONERA S3C3D + Catset	Plasma–fluid model for DBD FRSD using a numerical–analytical approach
[122]	Dimensional	2D	PASSKEY	Plasma–fluid model for DBD FRSD using a numerical approach
[121]	Dimensional	2D	In-house FEM	Transient plasma model focused on charge separation and EHD force

4. Discussion

1. Physical Representation of the Plasma–Flow Interaction.

One of the principal distinctions among phenomenological models for dielectric barrier discharge (DBD) plasma actuators lies in the manner in which the electrohydrodynamic (EHD) body force is represented. Although all formulations pursue the same objective—reproducing the macroscopic influence of plasma actuation on the surrounding flow—they differ substantially in the level of physical detail incorporated into the numerical description. Consequently, the evolution of these models reflects a progressive shift from simplified engineering approximations toward formulations that preserve a larger fraction of the underlying plasma physics without reaching the complexity of fully coupled plasma-fluid simulations.

The Shyy model represents the simplest physical approximation among the most widely adopted phenomenological approaches. By introducing the plasma effect directly as a prescribed momentum source within the Navier–Stokes equations, the formulation neglects the explicit solution of electrostatic variables, including charge transport and electric potential distributions. Despite these simplifications, the reviewed studies consistently demonstrate that the model successfully reproduces the dominant macroscopic effects of DBD actuation, such as wall-jet generation, boundary-layer energization, flow reattachment, and vortex attenuation. This observation suggests that, for many aerodynamic applications, accurate prediction of the detailed plasma discharge is not a prerequisite for obtaining reliable estimates of the resulting flow modification. Instead, the global momentum transfer appears to be the governing mechanism controlling the aerodynamic response.

The Suzen–Huang formulation introduces a significantly higher level of physical consistency by explicitly coupling the fluid solver with electrostatic equations governing electric potential and charge density. This additional physics enables the body force to emerge from the calculated electric field rather than from an imposed analytical distribution, providing a more realistic representation of the discharge region. As evidenced throughout the reviewed literature, subsequent developments have primarily focused on refining charge-density estimation, plasma-length prediction, and boundary-condition treatment rather than modifying the original theoretical framework. This evolution indicates that the fundamental structure of the Suzen–Huang model has proven sufficiently robust, with recent improvements directed toward reducing empirical dependence while preserving computational tractability. Consequently, the model occupies an intermediate position between simplified momentum-source formulations and fully resolved plasma-fluid approaches.

A fundamentally different philosophy is adopted by the Dörr–Kloker empirical model, in which the body-force distribution is reconstructed directly from experimentally measured velocity fields instead of being derived from electrostatic assumptions. Rather than increasing the physical complexity of the governing equations, this methodology transfers the physical realism to the experimental reconstruction process. As a result, the model naturally incorporates discharge characteristics and force distributions that may be difficult to reproduce using simplified analytical formulations. The reviewed investigations consistently report superior agreement with experimentally measured velocity fields, particularly within the plasma region where conventional phenomenological models tend to oversimplify the force distribution. However, this improved local accuracy is achieved at the expense of generality, since the predictive capability of the model becomes intrinsically dependent on the availability and quality of experimental calibration data.

Beyond these three reference formulations, physically based plasma-fluid models represent the highest level of physical fidelity currently available. Unlike phenomenological approaches, they directly resolve plasma generation, charged-species transport, electric-field evolution, and momentum exchange with the neutral fluid. These models therefore provide the most comprehensive description of DBD actuator operation and constitute the reference framework against which reduced-order formulations are commonly assessed. Nevertheless, their computational requirements remain prohibitive for most engineering-scale simulations, limiting their application primarily to fundamental plasma studies and model development.

The emergence of hybrid and reduced-order formulations illustrates a recent shift in modeling philosophy. Instead of pursuing either maximum physical fidelity or maximum numerical simplicity, these approaches seek to preserve only the dominant mechanisms governing plasma-induced momentum transfer while replacing computationally expensive processes with analytical approximations, experimental correlations, or simplified electrical models. This trend reflects the growing recognition that engineering-oriented simulations require an appropriate balance between physical realism and computational efficiency rather than a complete description of discharge physics.

Overall, the reviewed literature demonstrates that the progression of phenomenological modeling has not followed a linear path toward increasingly complex formulations. Instead, different models have evolved to satisfy different levels of physical representation according to their intended application. Simplified body-force models remain highly effective when the objective is predicting the global aerodynamic response, whereas electrostatic formulations become advantageous when the spatial distribution of the EHD force plays a dominant role. Empirical approaches offer the highest agreement with experimental observations whenever reliable calibration data are available, while plasma-fluid models continue to provide the benchmark for physical understanding. Consequently, the choice of an appropriate phenomenological model should not be interpreted as a competition between formulations but rather as the selection of the level of physical fidelity required to accurately reproduce the relevant flow phenomena.

2. Computational Efficiency and Numerical Complexity.

Computational efficiency remains one of the decisive criteria governing the selection of a phenomenological model for dielectric barrier discharge (DBD) plasma actuator simulations. Although all reviewed formulations seek to reproduce the electrohydrodynamic forcing generated by the discharge, they differ substantially in the number of additional equations solved, the required spatial resolution, and the sensitivity of the numerical procedure to operating conditions. Consequently, the literature reveals a clear trade-off between physical fidelity and computational cost, with each modeling strategy occupying a distinct position along this spectrum.

Among the commonly used formulations, the Shyy model consistently exhibits the lowest numerical complexity. Because the plasma effect is represented through a prescribed momentum source directly incorporated into the Navier–Stokes equations, the method does not require the solution of electrostatic variables or charged-species transport equations. As a result, the additional computational overhead remains relatively small compared with a baseline aerodynamic simulation. The reviewed studies repeatedly identify this simplicity as the principal reason for the widespread adoption of the Shyy formulation in large-scale engineering problems involving airfoils, turbomachinery, and aerothermal systems. Even when compared directly with more elaborate phenomenological approaches under identical flow conditions, the model generally converges with fewer iterations and reduced execution time while preserving comparable aerodynamic predictions.

The Suzen–Huang formulation introduces a moderate increase in computational demand because the electric potential and charge-density fields must be solved in addition to the flow equations. This coupling improves the physical representation of the discharge region but inevitably increases memory requirements, solver complexity, and sensitivity to boundary-condition treatment. Nevertheless, the available evidence indicates that the additional cost remains manageable for engineering-scale simulations and is significantly lower than that associated with fully coupled plasma-fluid models. For this reason, the Suzen–Huang approach is frequently selected when the spatial distribution of the electrohydrodynamic force is important, but the computational resources required by detailed plasma simulations are not available.

The Dörr–Kloker empirical methodology presents a different computational profile. Once the body-force distribution has been reconstructed from experimental data, the subsequent flow simulation can be performed with a computational effort comparable to that of simplified phenomenological models because no additional electrostatic equations are solved during runtime. However, this apparent efficiency conceals an important practical limitation: the force reconstruction process itself requires high-quality experimental measurements and additional preprocessing before numerical simulations can be conducted. Consequently, the overall modeling workflow may become more demanding than that of purely analytical formulations, particularly when multiple actuator configurations or operating conditions must be investigated.

Physically based plasma-fluid models represent the opposite extreme of the complexity spectrum. These formulations simultaneously resolve electric-field evolution, charged-species transport, plasma chemistry, and fluid dynamics across widely disparate temporal and spatial scales. The resulting systems are strongly coupled and highly stiff, requiring very small time steps and fine mesh resolution near the electrodes. The reviewed studies consistently emphasize that such models remain computationally prohibitive for most practical aerodynamic applications and are, therefore, used primarily for fundamental investigations, actuator characterization, and the generation of reference datasets for reduced-order formulations.

The emergence of reduced-order and hybrid approaches can be interpreted as a direct response to this computational challenge. By replacing the most expensive plasma processes with analytical approximations, empirical correlations, or simplified electrical representations, these methods seek to retain the dominant effects of plasma-induced momentum transfer while drastically reducing computational requirements. Their growing adoption in optimization studies, thermal-management analyses, and multiphysics simulations demonstrates that numerical efficiency has become as important as physical accuracy in contemporary plasma-actuator research.

Overall, the reviewed literature demonstrates that computational complexity increases systematically with the level of physical detail incorporated into the model. Simplified momentum-source formulations provide the highest efficiency and remain the preferred choice for extensive parametric studies and industrial-scale simulations. Electrostatic formulations offer an intermediate compromise between accuracy and cost, whereas empirical approaches shift part of the computational burden to the experimental calibration stage. Fully resolved plasma-fluid models, despite their superior physical fidelity, remain restricted to specialized investigations because of their substantial computational requirements. Consequently, the selection of a phenomenological model is fundamentally an exercise in balancing the desired level of physical realism against the available computational resources and the scale of the engineering problem under consideration.

3. Predictive Capability and Experimental Validation.

Beyond physical representation and computational efficiency, the predictive capability of phenomenological models constitutes one of the primary criteria for evaluating their suitability in engineering applications. Regardless of the underlying formulation, an effective plasma actuator model must accurately reproduce the macroscopic consequences of electrohydrodynamic forcing, including wall-jet development, boundary-layer modification, flow separation control, and the resulting aerodynamic performance. The reviewed literature demonstrates that, although the different phenomenological approaches employ substantially different physical assumptions, they generally converge toward comparable predictions of these global flow phenomena. Their principal differences emerge instead in the accuracy with which the spatial distribution of the body force and localized flow structures are represented.

The Shyy model has consistently demonstrated reliable predictive performance for engineering-scale aerodynamic simulations despite its simplified physical formulation. Numerous validation studies report that the model successfully reproduces the principal macroscopic effects of plasma actuation, including separation delay, lift enhancement, drag reduction, and vortex suppression across a broad range of flow configurations. Particularly noteworthy is the observation that its aerodynamic predictions often remain comparable to those obtained with more physically detailed formulations, despite requiring significantly fewer computational resources. This consistency suggests that, for many practical flow-control applications, the global momentum introduced by the actuator dominates the aerodynamic response, making simplified body-force representations sufficient for predicting integral performance parameters.

The Suzen–Huang formulation achieves similar predictive capability while providing improved representation of the electrohydrodynamic forcing process. Because the body force is derived from the calculated electric potential and charge-density fields, the model generally reproduces the spatial evolution of the plasma region with greater physical consistency. Validation against particle image velocimetry (PIV), schlieren imaging, and direct numerical simulations has demonstrated that the formulation accurately captures both steady and transient plasma-induced flow structures, including the formation and evolution of coherent vortices generated during burst-mode actuation. These studies further indicate that the model remains robust under a wide range of operating conditions, although its predictive accuracy depends on appropriate estimation of electrostatic parameters and careful treatment of boundary conditions. Consequently, the additional physical detail primarily improves the local representation of plasma forcing rather than fundamentally altering the predicted global aerodynamic trends.

The empirical Dörr–Kloker methodology exhibits the highest level of agreement with experimentally measured velocity fields because the body-force distribution is reconstructed directly from experimental observations. Unlike analytical formulations, which necessarily rely on simplifying assumptions regarding the plasma discharge, the empirical approach inherently incorporates complex physical effects present during actuator operation. This characteristic enables particularly accurate reproduction of the near-wall velocity distribution and localized momentum transfer within the discharge region. However, this superior agreement should not be interpreted as universally greater predictive capability. Since the reconstructed force field remains closely tied to the experimental conditions used during calibration, the model may lose accuracy when extrapolated to different actuator geometries, operating voltages, or flow environments for which no experimental information is available.

The reviewed literature also reveals an important distinction between validation and prediction. While empirical models achieve excellent agreement under calibrated conditions, electrostatic formulations such as Suzen–Huang generally offer greater flexibility for evaluating previously unexplored operating scenarios because the body force is generated from physically based governing equations rather than reconstructed data. Similarly, although the Shyy model incorporates a simplified force distribution, its robustness across diverse engineering applications demonstrates considerable predictive generality when the primary objective is evaluating global aerodynamic performance. This distinction highlights that predictive capability should not be assessed exclusively by agreement with existing experiments but also by the ability of a formulation to provide reliable estimates under new conditions where experimental measurements are unavailable.

Physically based plasma-fluid models continue to provide the benchmark for validation because they resolve the fundamental discharge mechanisms responsible for electrohydrodynamic force generation. Their ability to predict charge transport, electric-field evolution, and transient plasma behavior makes them invaluable for understanding the underlying physics and evaluating the assumptions adopted by reduced-order formulations. Nevertheless, their extensive computational requirements limit their routine use as predictive engineering tools, reinforcing their role as reference models for validation rather than practical simulation platforms.

Overall, the comparative evidence indicates that no phenomenological formulation demonstrates universally superior predictive capability across all performance metrics. Instead, prediction accuracy depends strongly on the quantity of interest being evaluated. Simplified momentum-source models provide remarkably accurate estimates of global aerodynamic performance, electrostatic formulations improve the representation of local plasma physics and transient behavior, empirical approaches maximize agreement with experimentally observed flow fields, and plasma-fluid models offer the highest physical fidelity for fundamental investigations. Consequently, model validation should be interpreted within the context of the intended engineering application, recognizing that different formulations optimize different aspects of predictive performance rather than pursuing a single definition of accuracy.

4. Engineering Applicability.

The widespread adoption of phenomenological models for dielectric barrier discharge (DBD) plasma actuators has been largely driven by their ability to address engineering problems that would be computationally impractical using fully resolved plasma simulations. However, the reviewed literature demonstrates that the suitability of each formulation depends not only on its predictive capability but also on the specific objectives of the numerical investigation. Rather than identifying a universally superior approach, recent research increasingly recognizes that each phenomenological model occupies a distinct niche within the spectrum of engineering applications.

The Shyy formulation has become the preferred choice for large-scale computational fluid dynamics studies where computational efficiency, numerical robustness, and ease of implementation are primary considerations. Its simple momentum-source representation enables straightforward integration into commercial and open-source CFD solvers without requiring modifications to the underlying numerical framework. This versatility explains its successful application across a remarkably broad range of engineering problems, including aerodynamic flow control, compressor stability enhancement, aeroelasticity, film cooling, and thermal management. In these applications, the principal objective is typically to evaluate the global aerodynamic or thermal response rather than to investigate the detailed physics of plasma generation. Consequently, the simplified representation adopted by the Shyy model is generally sufficient to support engineering design, parametric analyses, and optimization studies involving numerous operating conditions or geometric configurations.

The Suzen–Huang model is particularly advantageous when a more physically consistent description of the plasma discharge is required without abandoning the computational feasibility necessary for engineering-scale simulations. Because the electrohydrodynamic body force is derived from electrostatic field calculations, the formulation provides additional insight into the spatial characteristics of plasma forcing and its interaction with complex flow structures. This capability has facilitated its extensive application in studies involving boundary-layer transition, transient plasma actuation, actuator optimization, and detailed investigations of electrohydrodynamic force distributions. The reviewed studies indicate that the additional computational cost associated with solving the electrostatic equations is often justified when the local characteristics of the plasma region play a significant role in determining overall system performance.

The engineering applicability of the Dörr–Kloker empirical methodology differs substantially from that of electrostatic formulations. Since the body-force distribution is reconstructed directly from experimental measurements, the model is particularly well suited for validation studies, high-fidelity numerical reproductions of laboratory experiments, and investigations where accurate representation of the near-wall velocity field is required. Its ability to reproduce experimentally observed force distributions with minimal simplifying assumptions makes it an effective tool for evaluating flow-control mechanisms and assessing the performance of alternative phenomenological formulations. Nevertheless, the dependence on experimental calibration limits its applicability to design-oriented studies involving new actuator geometries or operating conditions for which suitable experimental datasets are unavailable.

Physically based plasma-fluid models continue to occupy a fundamentally different role within plasma actuator research. Their primary contribution lies in improving the understanding of discharge physics, charge transport, electric-field evolution, and plasma-flow coupling rather than supporting routine engineering design. Accordingly, these models are predominantly employed for actuator development, fundamental plasma investigations, and the generation of reference solutions used to validate or improve reduced-order formulations. Their limited application to large-scale engineering systems reflects computational constraints rather than deficiencies in predictive capability.

The reviewed literature also demonstrates a growing diversification of application areas beyond conventional aerodynamic flow control. While early investigations focused primarily on delaying boundary-layer separation and increasing lift, recent studies have successfully extended phenomenological models to turbomachinery, aeroelastic control, thermal management, plasma-assisted combustion, fluid–structure interaction, and multi-physics optimization. This expansion illustrates that the governing mechanism represented by these models—namely, plasma-induced momentum transfer—is sufficiently general to influence a wide variety of transport phenomena. Consequently, the selection of a modeling strategy increasingly depends on the dominant physical processes governing the engineering system rather than on the traditional distinction between aerodynamic and non-aerodynamic applications.

An important trend emerging from the reviewed studies is that engineering applicability is becoming increasingly associated with model adaptability. Modern simulations frequently involve coupled physical processes, multidisciplinary optimization, and complex geometries that require numerical formulations capable of balancing robustness, flexibility, and computational efficiency. In this context, simplified phenomenological models continue to dominate industrial-oriented applications, whereas electrostatic, empirical, and hybrid approaches provide complementary capabilities whenever higher physical fidelity or experimental consistency becomes necessary. Overall, the comparative analysis indicates that the different phenomenological models should be viewed as complementary engineering tools rather than competing alternatives. Their practical value is determined by the requirements of the specific application, including the desired level of physical detail, the availability of computational resources, the existence of experimental calibration data, and the objectives of the numerical investigation. Consequently, the engineering relevance of a given formulation is defined less by its intrinsic complexity than by its ability to provide reliable and computationally efficient predictions for the problem under consideration.

5. Current Research Trends and Future Perspectives.

The comparative analysis of the reviewed phenomenological models reveals that the current evolution of DBD plasma actuator modeling is no longer driven by the pursuit of increasingly complex formulations, but rather by the search for an optimal balance between physical fidelity, computational efficiency, and engineering applicability. This transition reflects the growing maturity of the field, where the principal challenge is no longer demonstrating that plasma actuators can modify fluid flow, but developing numerical models capable of supporting reliable design and optimization of plasma-assisted technologies under realistic operating conditions.

One of the most evident research trends is the gradual convergence of phenomenological and physically based approaches. Early model development followed two largely independent directions: simplified body-force formulations focused on engineering applications, and plasma-fluid models aimed at understanding the discharge physics. Recent investigations increasingly attempt to bridge these approaches by incorporating physically meaningful information into reduced-order formulations while preserving computational tractability. This tendency has resulted in the development of hybrid models that combine simplified electrostatic descriptions, experimental correlations, analytical approximations, and reduced plasma representations. Rather than replacing existing phenomenological models, these strategies seek to enhance their predictive capability without introducing the computational burden associated with fully coupled plasma simulations.

Another important trend concerns the progressive reduction in empirical dependence. Although phenomenological formulations have traditionally relied on experimentally calibrated parameters, several recent studies focus on deriving charge density distributions, plasma length, body-force intensity, and electrical characteristics directly from physically based relationships. This evolution is particularly evident in modern implementations of the Suzen–Huang framework, where analytical parameter estimation has gradually replaced empirical adjustments. Similar efforts are observed in reduced-order formulations that establish explicit relationships between electrical operating conditions and plasma-induced momentum transfer. Such developments improve the generality of phenomenological models by extending their applicability beyond the specific conditions under which they were originally calibrated.

The literature also demonstrates a clear expansion in the range of engineering applications addressed by plasma actuator models. While early investigations concentrated almost exclusively on external aerodynamic flow control, contemporary research increasingly considers multidisciplinary problems involving turbomachinery, aeroelasticity, thermal management, combustion enhancement, and fluid–structure interaction. This diversification has imposed new modeling requirements because plasma actuation must now be coupled with heat transfer, chemical reactions, structural dynamics, and multiphase transport. Consequently, future phenomenological models will likely require greater flexibility to accommodate coupled multiphysics simulations while maintaining acceptable computational performance.

Another emerging direction involves the increasing role of optimization methodologies and high-throughput numerical analyses. Modern engineering design frequently requires the evaluation of hundreds or even thousands of operating conditions, actuator geometries, and electrical excitation parameters. Under these circumstances, computational efficiency becomes as important as physical accuracy. This requirement explains the growing interest in reduced-order formulations, surrogate models, and hybrid computational strategies capable of supporting optimization procedures without compromising the reliability of the predicted flow response. In this context, simplified phenomenological models are expected to remain indispensable because their low computational cost enables large parametric studies that remain inaccessible to fully resolved plasma-fluid simulations.

An equally important observation emerging from the reviewed literature is that future developments are unlikely to establish a single universal phenomenological model. Instead, the evidence suggests a progressive specialization of numerical formulations according to their intended application. Simplified body-force models will probably continue to dominate industrial-scale CFD analyses where computational efficiency is the primary concern. Electrostatic formulations are expected to remain valuable for investigations requiring improved representation of plasma-force distributions, whereas empirical methodologies will continue to serve as high-accuracy validation tools whenever experimental databases are available. Physically based plasma-fluid models, in turn, will retain their role as benchmark solutions for understanding discharge physics and validating reduced-order approaches.

Looking forward, we see that one of the most promising research directions lies in the integration of data-driven methodologies with conventional phenomenological formulations. The increasing availability of high-resolution experimental measurements, advanced diagnostic techniques, and high-fidelity numerical databases provides opportunities to develop adaptive models capable of dynamically adjusting body-force distributions according to operating conditions. Such approaches could significantly reduce the dependence on empirical calibration while preserving computational efficiency, thereby overcoming one of the principal limitations shared by current phenomenological models. Furthermore, advances in machine learning, reduced-order modeling, and physics-informed computational methods offer the potential to construct hybrid frameworks that combine the interpretability of physics-based formulations with the predictive capability of data-driven techniques.

Overall, the evolution of phenomenological modeling demonstrates that the field has entered a stage of methodological consolidation rather than conceptual competition. The reviewed formulations should, therefore, be regarded as complementary tools that address different levels of physical complexity and engineering requirements. Future progress will likely depend less on replacing existing models and more on integrating their respective strengths into flexible computational frameworks capable of delivering accurate, robust, and computationally efficient predictions across the increasingly diverse range of applications envisioned for DBD plasma actuators.

Table X provides a qualitative comparison of the key features and performance of the different plasma actuator models discussed in this review. The models are evaluated across several criteria, including physical fidelity, computational cost, experimental dependence, local electrohydrodynamic (EHD) force prediction, global aerodynamic prediction, industrial applicability, and typical applications. This comparative overview highlights the strengths and limitations of each modeling approach and serves as a practical guideline for selecting the most suitable model depending on the specific objectives of a given study.

Table 5 provides a qualitative comparison of the key features and performance of the different plasma actuator models discussed in this review. The models are evaluated across several criteria, including physical fidelity, computational cost, experimental dependence, local electrohydrodynamic (EHD) force prediction, global aerodynamic prediction, industrial applicability, and typical applications. This comparative overview highlights the strengths and limitations of each modeling approach and serves as a practical guideline for selecting the most suitable model depending on the specific objectives of a given study.

Table 5. Qualitative comparison of key features and performance across plasma actuator models.

Performance Assessment of DBD Plasma Simulation Models					
Criterion	**Shyy**	**Suzen–Huang**	**Dörr-Kloker**	**Plasma-Fluid**	**Hybrid**
Physical fidelity	●●	● ● ●	● ● ●●	● ● ● ● ●	● ● ●
Computational cost	Very Low	Moderate	Low-Moderate	Very High	Low
Experimental dependence	Low	Moderate	High	Low	Moderate
Local EHD force prediction	Moderate	High	Very High	Excellent	High
Global aerodynamic prediction	High	High	High	Excellent	High
Industrial applicability	Excellent	High	Moderate	Limited	Very High
Typical applications	CFD, turbomachinery	Flow control	Validation	Plasma physics	Optimization

5. Conclusions

This review has shown that numerical modeling has become an essential tool for the design and optimization of dielectric barrier discharge (DBD) plasma actuators. Rather than identifying a universally superior model, the literature demonstrates that each modeling strategy addresses a different level of physical fidelity and computational complexity. Macroscopic formulations remain the preferred choice for engineering-oriented CFD because of their favorable balance between accuracy and computational cost, whereas microscopic plasma-fluid models continue to provide the highest physical insight for understanding discharge mechanisms and validating simplified approaches. Consequently, model selection should be driven by the objectives of the analysis, ranging from rapid aerodynamic optimization to detailed plasma physics investigations.

The analysis of the reviewed literature also reveals that numerical simulations have successfully extended DBD plasma actuators beyond conventional flow-separation control toward applications involving turbomachinery, aeroelasticity, thermal management, and high-speed aerodynamics. These advances demonstrate that plasma-based active flow control has evolved from a laboratory concept into a promising enabling technology for future aerospace systems. Nevertheless, important challenges remain, particularly regarding actuator energy efficiency, long-term durability, large-scale implementation, and reliable model calibration under varying operating conditions.

Looking forward, we find that one of the most promising research directions lies in the integration of plasma actuator models with Artificial Intelligence (AI) and Digital Twin technologies. Machine learning techniques could be employed to develop reduced-order surrogate models capable of reproducing high-fidelity plasma simulations in real time, dramatically reducing computational requirements during design optimization. Likewise, AI-based optimization algorithms may enable autonomous tuning of actuator voltage, frequency, waveform, and placement according to changing flight conditions.

Digital Twins represent another emerging opportunity for plasma-assisted active flow control. By combining CFD models, experimental measurements, and onboard sensor data, Digital Twins could continuously update the virtual representation of an aircraft, allowing DBD actuators to be optimized adaptively throughout operation. Such an approach would enable predictive flow-control strategies, health monitoring of plasma actuators, fault detection, and real-time aerodynamic optimization within next-generation autonomous aircraft.

Finally, future research is expected to move toward hybrid multiscale frameworks that combine physics-based plasma models, data-driven approaches, and real-time control architectures. The convergence of high-fidelity numerical simulations, artificial intelligence, advanced sensing technologies, and Digital Twins has the potential to transform DBD plasma actuators from primarily offline design tools into intelligent adaptive systems capable of continuously optimizing aerodynamic performance throughout the aircraft operational envelope.

Author Contributions: Conceptualization, J.F.I.Y. and V.M.C.; methodology, J.F.I.Y. and J.L.R.M.; formal analysis, V.M.C., A.S.H. and A.R.T.; investigation and resources, A.R.T. and J.L.R.M.; writing—original draft preparation, J.F.I.Y., V.M.C. and A.S.H.; supervision, V.M.C. All authors have read and agreed to the published version of the manuscript.

Funding: This research received no external funding.

Data Availability Statement: Data sharing is not applicable. No new data were created or analyzed in this study.

Conflicts of Interest: The authors declare no conflicts of interest.

References

1. Tsourdos, A. Flight control systems: Practical issues in design and implementation. *Proc. Inst. Mech. Eng.* **2000**, *214*, 323.
2. Moir, I.; Seabridge, A. *Aircraft Systems: Mechanical, Electrical, and Avionics Subsystems Integration*; John Wiley & Sons: Hoboken, NJ, USA, 2011.
3. Wang, S.; Tomovic, M.; Liu, H. Chapter 1-Requirements for the Hydraulic System of a Flight Control System. In *Commercial Aircraft Hydraulic Systems*; Wang, S., Tomovic, M., Liu, H., Eds.; Aerospace Engineering; Academic Press: Oxford, UK, 2016; pp. 1–52. [CrossRef]
4. Qiao, G.; Liu, G.; Shi, Z.; Wang, Y.; Ma, S.; Lim, T.C. A review of electromechanical actuators for More/All Electric aircraft systems. *Proc. Inst. Mech. Eng. Part C J. Mech. Eng. Sci.* **2018**, *232*, 4128–4151.
5. Frischemeier, S. Electrohydrostatic Actuators for Aircraft Primary Flight Control-Types, Modelling and Evaluation. 1997. Available online: https://tore.tuhh.de/dspace-cris-server/api/core/bitstreams/64ccde8a-24c6-47ac-a44d-10a4c209e455/content (accessed on 22 July 2026).
6. Altare, G.; Vacca, A.; Richter, C. A novel pump design for an efficient and compact Electro-Hydraulic Actuator IEEE aerospace conference. In *Proceedings of the 2014 IEEE Aerospace Conference*; IEEE: Piscataway, NJ, USA, 2014; pp. 1–12.
7. Navarro, R. Performance of an electro-hydrostatic actuator on the F-18 systems research aircraft. In *Proceedings of the 16th Digital Avionics Systems Conference*; Number NASA/TM-97-206224; NASA: Washington, DC, USA, 1997.
8. Alle, N.; Hiremath, S.S.; Makaram, S.; Subramaniam, K.; Talukdar, A. Review on electro hydrostatic actuator for flight control. *Int. J. Fluid Power* **2016**, *17*, 125–145. [CrossRef]
9. Edge, J. *An Electromechanical Actuator Technology Development Program*; Technical Report; SAE Technical Paper; SAE: Warrendale, PA, USA, 1978.
10. Kang, K.; Pachter, M.; Houpis, C.; Rasmussen, S. Modeling and control of an electro-hydrostatic actuator. In Proceedings of the IEEE 1995 National Aerospace and Electronics Conference (NAECON 1995); IEEE: Piscataway, NJ, USA, 1995; Volume 1, pp. 545–556.
11. Rubertus, D.P.; Hunter, L.D.; Cecere, J. Electromechanical actuation technology for the all-electric aircraft. *IEEE Trans. Aerosp. Electron. Syst.* **1984**, 243–249. [CrossRef]
12. Albright, J.; Moore, L. Development and implementation of electromechanical actuators for the X-38 atmospheric test vehicles. In Proceedings of the AIAA Atmospheric Flight Mechanics Conference and Exhibit, Honolulu, HI, USA, 18–21 August 2008; p. 6569.

13. Di Rito, G.; Galatolo, R.; Schettini, F. Self-monitoring electro-mechanical actuator for medium altitude long endurance unmanned aerial vehicle flight controls. *Adv. Mech. Eng.* **2016**, *8*, 1687814016644576. [CrossRef]
14. Fu, J.; Maré, J.C.; Fu, Y. Modelling and simulation of flight control electromechanical actuators with special focus on model architecting, multidisciplinary effects and power flows. *Chin. J. Aeronaut.* **2017**, *30*, 47–65. [CrossRef]
15. Villani, M.; Tursini, M.; Fabri, G.; Castellini, L. Electromechanical actuator for helicopter rotor damper application. *IEEE Trans. Ind. Appl.* **2013**, *50*, 1007–1014. [CrossRef]
16. Giangrande, P.; Galassini, A.; Papadopoulos, S.; Al-Timimy, A.; Calzo, G.L.; Degano, M.; Galea, M.; Gerada, C. Considerations on the development of an electric drive for a secondary flight control electromechanical actuator. *IEEE Trans. Ind. Appl.* **2019**, *55*, 3544–3554. [CrossRef]
17. Schallert, C. Concept for the Design of Flight Control Actuation and Laws for Future All-Electric Aircraft. *IFAC Proc. Vol.* **2007**, *40*, 67–72. [CrossRef]
18. Chakraborty, I.; Trawick, D.R.; Jackson, D.; Mavris, D. Electric control surface actuator design optimization and allocation for the more electric aircraft. In Proceedings of the 2013 Aviation Technology, Integration, and Operations Conference, Los Angeles, CA, USA, 12–14 August 2013; p. 4283.
19. Vanek, B.; Szabó, Z.; Edelmayer, A.; Bokor, J. Fault detection of electrical flight control system actuators using parameter dependent estimation*. *IFAC Proc. Vol.* **2012**, *45*, 1358–1363. [CrossRef]
20. Jensen, S.C.; Jenney, G.D.; Dawson, D. Flight test experience with an electromechanical actuator on the F-18 systems research aircraft. In *Proceedings of the 19th Digital Avionics Systems Conference*; Proceedings (Cat. No. 00CH37126); IEEE: Piscataway, NJ, USA, 2000; Volume 1, p. 2E3-1.
21. Derrien, J.C.; Sécurité, S.D. Electromechanical actuator (EMA) advanced technologies for flight controls. In Proceedings of the International Congress of the Aeronautical Sciences, Brisbane, Australia, 23–28 September 2012; pp. 1–10.
22. Sinnett, M. Boeing 787 No-Bleed Systems: Saving Fuel and Enhancing Operational Efficiencies. 2007. Available online: https://www.semanticscholar.org/paper/Aero-Quarterly-Qtr_04-%7C-07-787-No-bleed-Systems%3A-Sinnett/4ba258aba7c71d54c705523dbddfd6e3e86954ed (accessed on 22 July 2026).
23. Todeschi, M. Airbus-EMAs for flight controls actuation system 2012 status and perspectives. In *Proceedings of the 5th International Conference on Recent Advances in Aerospace Actuation Systems and Components*; SAE International: Warrendale, PA, USA, 2012; p. 1. Available online: https://legacy.sae.org/publications/technical-papers/content/2011-01-2732/ (accessed on 22 July 2026).
24. Norton, W.J. *Advanced Electromechanical Actuation System (EMAS), Flight Test*; Technical Report, TEST WING (4950TH) WRIGHT-PATTERSON AFB OH; Defense Technical Information Center (DTIC): Fort Belvoir, VA, USA, 1986.
25. Derrien, J.C.; Tieys, P.; Senegas, D.; Todeschi, M. *Ema Aileron Covadis Development*; Technical Report; SAE Technical Paper; SAE: Warrendale, PA, USA, 2011.
26. Mazzoleni, M.; Maccarana, Y.; Previdi, F.; Pispola, G.; Nardi, M.; Perni, F.; Toro, S. Development of a reliable electro-mechanical actuator for primary control surfaces in small aircrafts. In *Proceedings of the 2017 IEEE International Conference on Advanced Intelligent Mechatronics (AIM)*; IEEE: Piscataway, NJ, USA, 2017; pp. 1142–1147.
27. Mazzoleni, M.; Previdi, F.; Scandella, M.; Pispola, G. Experimental development of a health monitoring method for electro-mechanical actuators of flight control primary surfaces in more electric aircrafts. *IEEE Access* **2019**, *7*, 153618–153634. [CrossRef]
28. Di Rito, G.; Luciano, B.; Borgarelli, N.; Nardeschi, M. Motor speed reconstruction in a compact EMA for primary flight controls via sensor-fusion technique. In *Proceedings of the 2021 IEEE 8th International Workshop on Metrology for AeroSpace (MetroAeroSpace)*; IEEE: Piscataway, NJ, USA, 2021; pp. 42–47.
29. Sutherland, J. *Fly-by-Wire Flight Control Systems*; Technical Report; Air Force Flight Dynamics Lab: Dayton, OH, USA, 1968.
30. Collinson, R. Fly-by-wire flight control. In *Introduction to Avionics Systems*; Springer: Cham, Switzerland, 2011; pp. 179–253.
31. Wilkinson, L.; Watson, D.; Page, R.; Organ, R. *The Story of the Avro Arrow from its Evolution to its Extinction*; Boston Mills Press: Erin, ON, Canada, 1980.
32. Nicolin, I.; Nicolin, B.A. The fly-by-wire system. *Incas Bull.* **2019**, *11*, 217–222. [CrossRef]
33. Tomayko, J.E. *Computers Take Flight: A History of NASA's Pioneering Digital Fly-by-Wire Project*; United States Government Printing: Washington, DC, USA, 2000.
34. Szalai, K.; Felleman, P.; Gera, J.; Glover, R. Design and test experience with a triply redundant digital fly-by-wire control system. In Proceedings of the Guidance and Control Conference, San Diego, CA, USA, 16–18 August 1976; p. 1911.
35. Jarvis, C.R. *Operational Experience with the Electronic Flight Control Systems of a Lunar-Landing Research Vehicle*; Technical Report; NASA: Washington, DC, USA, 1966.
36. Hodge, K.E.; Kellogg, Y. *Proceedings of the F-8 Digital Fly-by-Wire and Supercritical Wing First Flight's 20th Anniversary Celebration*; Technical Report; NASA: Washington, DC, USA, 1996.
37. Naayagi, R. A review of more electric aircraft technology. In *Proceedings of the 2013 International Conference on Energy Efficient Technologies for Sustainability*; IEEE: Piscataway, NJ, USA, 2013; pp. 750–753.
38. Dugan, J.B.; Van Buren, R. Reliability evaluation of fly-by-wire computer systems. *J. Syst. Softw.* **1994**, *25*, 109–120. [CrossRef]

39. Corps, S. Airbus A320 Side Stick and Fly by Wire—An Update. In *SAE Transactions*; SAE: Warrendale, PA, USA, 1986; pp. 1263–1275.
40. Garg, A.; Linda, R.I.; Chowdhury, T. Evolution of aircraft flight control system and fly-by-light flight control system. *Int. J. Emerg. Technol. Adv. Eng.* **2013**, *3*, 61–63.
41. Brière, D.; Traverse, P. AIRBUS A320/A330/A340 electrical flight controls-A family of fault-tolerant systems. In *Proceedings of the FTCS-23 The Twenty-Third International Symposium on Fault-Tolerant Computing*; IEEE: Piscataway, NJ, USA, 1993; pp. 616–623.
42. Neretti, G. Active flow control by using plasma actuators. In *Recent Progress in Some Aircraft Technologies*; IntechOpen: London, UK, 2016; pp. 57–76.
43. Gu, X.; Duc Vo, H.; Mureithi, N.W.; Laurendeau, E. Plasma Gurney Flap Flight Control at Low Angle of Attack. *J. Aircr.* **2023**, *60*, 172–189. [CrossRef]
44. Roth, J.; Sherman, D.; Wilkinson, S. Boundary layer flow control with a one atmosphere uniform glow discharge surface plasma. In Proceedings of the 36th AIAA Aerospace Sciences Meeting and Exhibit, Reno, NV, USA, 12–15 January 1998; p. 328.
45. Bénard, N.; Jolibois, J.; Moreau, E. Lift and drag performances of an axisymmetric airfoil controlled by plasma actuator. *J. Electrost.* **2009**, *67*, 133–139. [CrossRef]
46. Aono, H.; Yamakawa, S.; Iwamura, K.; Honami, S.; Ishikawa, H. Straight and curved type micro dielectric barrier discharge plasma actuators for active flow control. *Exp. Therm. Fluid Sci.* **2017**, *88*, 16–23. [CrossRef]
47. Hajipour, M.; Ebrahimi, A.; Amandolese, X. Active flow control of a wing section in stall flutter by dielectric barrier discharge plasma actuators. *Phys. Fluids* **2022**, *34*, 077107. [CrossRef]
48. Corke, T.C.; Post, M.L.; Orlov, D.M. SDBD plasma enhanced aerodynamics: Concepts, optimization and applications. *Prog. Aerosp. Sci.* **2007**, *43*, 193–217. [CrossRef]
49. Pescini, E.; Francioso, L.; De Giorgi, M.G.; Ficarella, A. Investigation of a micro dielectric barrier discharge plasma actuator for regional aircraft active flow control. *IEEE Trans. Plasma Sci.* **2015**, *43*, 3668–3680. [CrossRef]
50. Vaddi, R.S.; Sota, C.; Mamishev, A.; Novosselov, I. Active Flow Control of NACA 0012 airfoil using Sawtooth Direct Current Augmented Dielectric Barrier Discharge Plasma Actuator. *arXiv* **2021**, arXiv:2106.11453.
51. Altıntaş, A.; Davidson, L.; Peng, S.H. Direct numerical simulation of drag reduction by spanwise oscillating dielectric barrier discharge plasma force. *Phys. Fluids* **2020**, *32*, 075101. [CrossRef]
52. Ji, S.; Zhang, B.; Li, J.; Wang, G. Numerical Study for Active Flow Control Using Dielectric Barrier Discharge Actuators. *J. Aerosp. Eng.* **2017**, *30*, 04017050. [CrossRef]
53. Yang, P.; Zhang, X.; Lai, Q.; Che, B.; Chen, L. Experimental investigation of the influence of scaling effects of wings on the flow separation control using plasma actuators. *Chin. J. Theor. Appl. Mech.* **2021**, *53*, 3321–3330.
54. Zhao, G.Y.; Li, Y.H.; Hua, W.Z.; Liang, H.; Han, M.H.; Niu, Z.G. Experimental study of flow control on delta wings with different sweep angles using pulsed nanosecond DBD plasma actuators. *Proc. Inst. Mech. Eng. Part G J. Aerosp. Eng.* **2015**, *229*, 1966–1974.
55. Kesuma, M.D.; Irwansyah, R.; Julian, J.; Satyadharma, D. Flow control with multi-dbd plasma actuator on a delta wing. *Evergreen* **2020**, *7*, 602–608. [CrossRef]
56. Sung, Y.; Kim, W.; Mungal, M.; Cappelli, M. Aerodynamic modification of flow over bluff objects by plasma actuation. *Exp. Fluids* **2006**, *41*, 479–486. [CrossRef]
57. Thomas, F.; Kozlov, A.; Corke, T. Plasma actuators for bluff body flow control. In Proceedings of the 3rd AIAA Flow Control Conference, San Francisco, CA, USA, 5–8 June 2006; p. 2845.
58. He, C.; Corke, T.C.; Patel, M.P. Plasma flaps and slats: An application of weakly ionized plasma actuators. *J. Aircr.* **2009**, *46*, 864–873. [CrossRef]
59. Corke, T.; Jumper, E.; Post, M.; Orlov, D.; McLaughlin, T. Application of weakly-ionized plasmas as wing flow-control devices. In Proceedings of the 40th AIAA Aerospace Sciences Meeting & Exhibit, Reno, NV, USA, 14–17 January 2002; p. 350.
60. Boesch, G.; Vo, H.D.; Savard, B.; Wanko-Tchatchouang, C.; Mureithi, N.W. Flight control using wing-tip plasma actuation. *J. Aircr.* **2010**, *47*, 1836–1846. [CrossRef]
61. Patel, M.P.; Ng, T.T.; Vasudevan, S.; Corke, T.C.; He, C. Plasma actuators for hingeless aerodynamic control of an unmanned air vehicle. *J. Aircr.* **2007**, *44*, 1264–1274. [CrossRef]
62. Wang, J.J.; Choi, K.S.; Feng, L.H.; Jukes, T.N.; Whalley, R.D. Recent developments in DBD plasma flow control. *Prog. Aerosp. Sci.* **2013**, *62*, 52–78. [CrossRef]
63. Jayaraman, B.; Shyy, W. Modeling of dielectric barrier discharge-induced fluid dynamics and heat transfer. *Prog. Aerosp. Sci.* **2008**, *44*, 139–191. [CrossRef]
64. Corke, T.C.; Enloe, C.L.; Wilkinson, S.P. Dielectric barrier discharge plasma actuators for flow control. *Annu. Rev. Fluid Mech.* **2010**, *42*, 505–529. [CrossRef]
65. Cho, Y.C.; Shyy, W. Adaptive flow control of low-Reynolds number aerodynamics using dielectric barrier discharge actuator. *Prog. Aerosp. Sci.* **2011**, *47*, 495–521. [CrossRef]

66. Portugal, S.; Choudhury, B.; Cardenas, D. Advances on aerodynamic actuation induced by surface dielectric barrier discharges. *Front. Phys.* **2022**, *10*, 923103. [CrossRef]
67. Zhang, X.; Yugang, Z.; Chun, Y. Recent developments in thermal characteristics of surface dielectric barrier discharge plasma actuators driven by sinusoidal high-voltage power. *Chin. J. Aeronaut.* **2023**, *36*, 1–21. [CrossRef]
68. Shyy, W.; Jayaraman, B.; Andersson, A. Modeling of glow discharge-induced fluid dynamics. *J. Appl. Phys.* **2002**, *92*, 6434–6443. [CrossRef]
69. Bernal-Orozco, R.A.; Carvajal-Mariscal, I.; Huerta-Chavez, O.M. Performance of DBD Actuator Models under Various Operating Parameters and Modifications to Improve Them. *Fluids* **2023**, *8*, 112. [CrossRef]
70. Adamiak, K. Quasi-stationary modeling of the DBD plasma flow control around airfoil. *Phys. Fluids* **2020**, *32*, 085108. [CrossRef]
71. Suzen, Y.; Huang, G.; Jacob, J.; Ashpis, D. Numerical Simulations of Plasma Based Flow Control Applications. In *Proceedings of the 35th AIAA Fluid Dynamics Conference and Exhibit*; AIAA: Reston, VA, USA, 2012; pp. 1–11. [CrossRef]
72. Suzen, Y.; Huang, G. Simulations of flow separation control using plasma actuators. In Proceedings of the 44th AIAA Aerospace Sciences Meeting and Exhibit, Reno, NV, USA, 9–12 January 2006; p. 877.
73. Seth, U.; Traoré, P.; Duran-Olivencia, F.; Moreau, E.; Vazquez, P. Parametric study of a DBD plasma actuation based on the Suzen-Huang model. *J. Electrost.* **2018**, *93*, 1–9. [CrossRef]
74. Ibrahim, I.; Skote, M. Modeling the plasma actuator via the splitting of the electric potential. In Proceedings of the Icms2010: Proceedings of the Third International Conference on Modelling and Simulation, Gaborone, Botswana, 6–8 September 2010; Volume 2, pp. 1–6.
75. Ibrahim, I.; Skote, M. Simulations of the linear plasma synthetic jet actuator utilizing a modified Suzen-Huang model. *Phys. Fluids* **2012**, *24*, 113602. [CrossRef]
76. Halimi Bin Ibrahim, I.; Skote, M. Effects of the scalar parameters in the Suzen-Huang model on plasma actuator characteristics. *Int. J. Numer. Methods Heat Fluid Flow* **2013**, *23*, 1076–1103. [CrossRef]
77. Ibrahim, I.H.; Skote, M. Boundary Condition Modifications of the Suzen-Huang Plasma Actuator Model. *Int. J. Flow Control* **2011**, *3*, 111–132. [CrossRef]
78. Lieberman, M.A. *A Mini-Course on the Principles of Plasma Discharges*; University of California: Berkley, CA, USA, 2003.
79. Ibrahim, I.; Skote, M. Simulating plasma actuators in a channel flow configuration by utilizing the modified Suzen-Huang model. *Comput. Fluids* **2014**, *99*, 144–155. [CrossRef]
80. Enloe, C.; McLaughlin, T.E.; VanDyken, R.D.; Kachner, K.; Jumper, E.J.; Corke, T.C. Mechanisms and responses of a single dielectric barrier plasma actuator: Plasma morphology. *AIAA J.* **2004**, *42*, 589–594. [CrossRef]
81. Enloe, C.; McLaughlin, T.E.; Font, G.; Baughn, J. Parameterization of temporal structure in the single-dielectric-barrier aerodynamic plasma actuator. *AIAA J.* **2006**, *44*, 1127–1136. [CrossRef]
82. Enloe, C.; McLaughlin, T.; Van Dyken, R.; Fischer, J. Plasma structure in the aerodynamic plasma actuator. In Proceedings of the 42nd AIAA Aerospace Sciences Meeting and Exhibit, Reno, NV, USA, 5–8 January 2004; p. 844.
83. Dörr, P.C.; Kloker, M.J. Numerical investigation of plasma-actuator force-term estimations from flow experiments. *J. Phys. D Appl. Phys.* **2015**, *48*, 395203. [CrossRef]
84. Maden, I.; Maduta, R.; Kriegseis, J.; Jakirlić, S.; Schwarz, C.; Grundmann, S.; Tropea, C. Experimental and computational study of the flow induced by a plasma actuator. *Int. J. Heat Fluid Flow* **2013**, *41*, 80–89. [CrossRef]
85. Bernal-Orozco, R.; Arias-Montano, A.; Huerta-Chávez, O. Separated-Flow Control Simulation with a Periodic Excitation by SDBD Plasma Actuator at Re= O (20 5). *J. Aerosp. Eng.* **2020**, *33*, 05020003. [CrossRef]
86. Roth, J. Electrohydrodynamically induced airflow in a one atmosphere uniform glow discharge surface plasma. In *Proceedings of the 25th Anniversary, IEEE Conference Record-Abstracts. 1998 IEEE International Conference on Plasma Science (Cat. No. 98CH36221)*; IEEE: Piscataway, NJ, USA, 1998; p. 291.
87. Orlov, D.; Corke, T. Numerical simulation of aerodynamic plasma actuator effects. In Proceedings of the 43rd AIAA Aerospace Sciences Meeting and Exhibit, Reno, NV, USA, 10–13 January 2005; p. 1083.
88. Massines, F.; Rabehi, A.; Decomps, P.; Gadri, R.B.; Ségur, P.; Mayoux, C. Experimental and theoretical study of a glow discharge at atmospheric pressure controlled by dielectric barrier. *J. Appl. Phys.* **1998**, *83*, 2950–2957. [CrossRef]
89. Boeuf, J.; Pitchford, L. Electrohydrodynamic force and aerodynamic flow acceleration in surface dielectric barrier discharge. *J. Appl. Phys.* **2005**, *97*, 103307. [CrossRef]
90. Rouffet, J.B.; Tech, S.H.; du Grand Noble, Z. Plasma actuator influence on air flow. In Proceedings of the COMSOL Conference 2008, Hannover, Germany, 1–9 October 2008.
91. Abdelraouf, H.; Elmekawy, A.M.N.; Kassab, S.Z. Simulations of flow separation control numerically using different plasma actuator models. *Alex. Eng. J.* **2020**, *59*, 3881–3896. [CrossRef]
92. Hasan, M.; Atkinson, M. Investigation of a Dielectric Barrier Discharge Plasma Actuator to Control Turbulent Boundary Layer Separation. *Appl. Sci.* **2020**, *10*, 1911. [CrossRef]

93. Mahboubidoust, A.; Ramiar, A.; Dardel, M. Investigation of steady plasma actuation effect on aerodynamic coefficients of oscillating airfoil at low Reynolds number. *Theor. Appl. Mech. Lett.* **2017**, *7*, 185–198. [CrossRef]
94. Zheng, J.; Cui, Y.; Khoo, B. A comparative study of alternating current and nanosecond plasma actuators in flow separation control. *Int. J. Heat Mass Transf.* **2019**, *135*, 1097–1117. [CrossRef]
95. Anzalotta, C.; Joshi, K.; Fernandez, E.; Bhattacharya, S. Effect of forcing the tip-gap of a NACA0065 airfoil using plasma actuators: A proof-of-concept study. *Aerosp. Sci. Technol.* **2020**, *107*, 106268. [CrossRef]
96. Bagheri, H.; Mirjalily, S.A.A.; Oloomi, S.A.A.; Salimpour, M.R. Effects of flow momentum enhancement using an artificial external source on shock wave strength, a CFD study. *Acta Astronaut.* **2021**, *187*, 70–78. [CrossRef]
97. De Giorgi, M.G.; Motta, V.; Suma, A.; Laforì, A. Comparison of different plasma actuation strategies for aeroelastic control on a linear compressor cascade. *Aerosp. Sci. Technol.* **2021**, *117*, 106902. [CrossRef]
98. Benmoussa, A.; Páscoa, J.C. Cycloidal rotor coupled with DBD plasma actuators for performance improvement. *Aerosp. Sci. Technol.* **2021**, *110*, 106468. [CrossRef]
99. Khoshnejad, A.; Ebrahimi, R.; Pouryoussefi, S.G. Numerical investigation of plasma actuator induced forcing direction on the performance of a low-speed isolated axial compressor rotor. *J. Electrost.* **2022**, *118*, 103732. [CrossRef]
100. Li, G.; Wang, Q.; Huang, Y.; Zhang, H. Large eddy simulation of film cooling effectiveness on a turbine vane pressure side with a saw-tooth plasma actuator. *Aerosp. Sci. Technol.* **2021**, *112*, 106615. [CrossRef]
101. Li, G.; Huang, Y.; Zhang, H.; Yan, W.; Nie, D. Numerical comparison of saw-tooth plasma actuators for film cooling flow control over a flat plate. *Int. J. Therm. Sci.* **2021**, *163*, 106807. [CrossRef]
102. Sun, J.; Zhang, F.; Wang, J.; Xie, G.; Sundén, B. Effects of plasma actuation and hole configuration on film cooling performance. *Propuls. Power Res.* **2023**, *12*, 227–237. [CrossRef]
103. Abdollahzadeh, M.; Páscoa, J.; Oliveira, P. Modified split-potential model for modeling the effect of DBD plasma actuators in high altitude flow control. *Curr. Appl. Phys.* **2014**, *14*, 1160–1170. [CrossRef]
104. Omidi, J.; Mazaheri, K. Improving the performance of a numerical model to simulate the EHD interaction effect induced by dielectric barrier discharge. *Int. J. Heat Fluid Flow* **2017**, *67*, 79–94. [CrossRef]
105. Brauner, T.; Laizet, S.; Bernard, N.; Moreau, E. Modelling of Dielectric Barrier Discharge Plasma Actuators for Direct Numerical Simulations. In Proceedings of the 8th AIAA Flow Control Conference, Washington, DC, USA, 13–17 June 2016; pp. 1–17. [CrossRef]
106. Pescini, E.; Martínez, D.; De Giorgi, M.; Ficarella, A. Optimization of micro single dielectric barrier discharge plasma actuator models based on experimental velocity and body force fields. *Acta Astronaut.* **2015**, *116*, 318–332. [CrossRef]
107. Aono, H.; Sekimoto, S.; Sato, M.; Yakeno, A.; Nonomura, T.; Fujii, K. Computational and experimental analysis of flow structures induced by a plasma actuator with burst modulations in quiescent air. *Mech. Eng. J.* **2015**, *2*, 15-00233. [CrossRef]
108. Abdollahzadeh, M.; Rodrigues, F.; Pascoa, J.; Oliveira, P. Numerical design and analysis of a multi-DBD actuator configuration for the experimental testing of ACHEON nozzle model. *Aerosp. Sci. Technol.* **2015**, *41*, 259–273. [CrossRef]
109. Kadivar, A.; Amanifard, N.; Deylami, H.M.; Dolati, F. Flow separation control in an axial compressor cascade using various arrangement of plasma actuator. *J. Electrost.* **2021**, *112*, 103580. [CrossRef]
110. Mazaheri, K.; Omidi, J.; Kiani, K. Simulation of DBD plasma actuator effect on aerodynamic performance improvement using a modified phenomenological model. *Comput. Fluids* **2016**, *140*, 371–384. [CrossRef]
111. Karimi, S.; Mohammadikalakoo, B.; Schito, P. Performance enhancement of single dielectric barrier discharge flow control actuators by means of rear linking tunnels on a reference bluff body using CFD. *J. Wind. Eng. Ind. Aerodyn.* **2021**, *209*, 104488. [CrossRef]
112. Li, G.; Zhang, H.; Yan, W.; Liu, L. Large eddy simulation of film cooling flow from cylindrical hole with dielectric barrier discharge plasma actuators. *Appl. Therm. Eng.* **2019**, *155*, 277–288. [CrossRef]
113. Omidi, J.; Mazaheri, K. Aerodynamic Enhancement and Improving the Performance of a Six-Megawatt DOWEC Wind Turbine by Micro-Plasma Actuator. *Int. J. Mech. Sci.* **2021**, *195*, 106228. [CrossRef]
114. Kaparos, P.; Vlahostergios, Z.; Panagiotou, P.; Yakinthos, K. Drag Reduction in Aircraft Wings Using Dielectric Barrier Discharge (DBD) Plasma Flow Control Actuators. In Proceedings of the 2nd Environmentally Compatible Air Transport System (ECATS) Conference, Athens, Greece, 7–9 November 2016.
115. Dörr, P.C.; Kloker, M.J. Transition Control in a Three-dimensional Boundary-layer Flow Using Plasma Actuators. *Procedia IUTAM* **2015**, *14*, 469–478. [CrossRef]
116. Wang, Z.; Wang, L.; Wang, Q.; Xu, S.; Fu, S. Control of crossflow instability over a swept wing using dielectric-barrier-discharge plasma actuators. *Int. J. Heat Fluid Flow* **2018**, *73*, 209–222. [CrossRef]
117. Jayaraman, B.; Shyy, W.; Thakur, S. Modeling of dielectric barrier discharge and resulting fluid dynamics. In *Proceedings of the 44th AIAA Aerospace Sciences Meeting and Exhibit*; AIAA: Reston, VA, USA, 2016. [CrossRef]
118. Singh, K.P.; Roy, S. Force approximation for a plasma actuator operating in atmospheric air. *J. Appl. Phys.* **2008**, *103*, 013305. [CrossRef]

119. Papageorgiou, L.; Metaxas, A.C.; Georghiou, G.E. Three-dimensional numerical modelling of gas discharges at atmospheric pressure incorporating photoionization phenomena. *J. Phys. D Appl. Phys.* **2011**, *44*, 045203. [CrossRef]
120. Abdollahzadeh, M.; Pascoa, J.; Oliveira, P. Implementation of the classical plasma–fluid model for simulation of dielectric barrier discharge (DBD) actuators in OpenFOAM. *Comput. Fluids* **2016**, *128*, 77–90. [CrossRef]
121. Singh, K.P.; Roy, S. Simulation of an asymmetric single dielectric barrier plasma actuator. *J. Appl. Phys.* **2005**, *98*, 083303. [CrossRef]
122. Chen, X.; Zhu, Y.; Wu, Y.; Su, Z.; Liang, H. Modeling and theoretical analysis of SDBD plasma actuators driven by fast-rise–slow-decay pulsed-DC voltages. *J. Phys. D Appl. Phys.* **2020**, *53*, 465202. [CrossRef]
123. Kotsonis, M.; Ghaemi, S. Experimental and numerical characterization of a plasma actuator in continuous and pulsed actuation. *Sens. Actuators A Phys.* **2012**, *187*, 84–94. [CrossRef]
124. Kotsonis, M.; Ghaemi, S.; Veldhuis, L.; Scarano, F. Measurement of the body force field of plasma actuators. *J. Phys. D Appl. Phys.* **2011**, *44*, 045204. [CrossRef]
125. Yoon, J.S.; Han, J.H. One-equation modeling and validation of dielectric barrier discharge plasma actuator thrust. *J. Phys. D Appl. Phys.* **2014**, *47*, 405202. [CrossRef]
126. Szulga, N.; Vermeersch, O.; Forte, M.; Casalis, G. Experimental and Numerical Study of Boundary Layer Transition Control Over an Airfoil Using a DBD Plasma Actuator. *Procedia IUTAM* **2015**, *14*, 403–412. [CrossRef]
127. Liu, B.; Liang, H.; Han, Z.; Li, Y.; Liu, F.; Chi, J.; Ding, Z. Numerical research on airfoil transition delay by alternative current dielectric barrier discharge actuation. *Chin. J. Aeronaut.* **2021**, *34*, 441–453. [CrossRef]
128. Chen, K.; Wei, C.Y.; Shi, Z.W. Effect of NS-DBD Actuator Parameters on the Aerodynamic Performance of a Flap Lifting Device. *Appl. Sci.* **2019**, *9*, 5213. [CrossRef]
129. Sumanik, S.; Etele, J.; Pimentel, R. Novel numerical boundary condition for simulating plasma actuator effects on rocket roll rate. *Acta Astronaut.* **2019**, *162*, 555–562. [CrossRef]
130. Amanifard, N.; Abdollahzadeh, M.; Moayedi, H.; Pascoa, J. An explicit CFD model for the DBD plasma actuators using wall-jet similarity approach. *J. Electrost.* **2020**, *107*, 103497. [CrossRef]
131. Erfani, R.; Erfani, T.; Utyuzhnikov, S.V.; Kontis, K. Optimisation of multiple encapsulated electrode plasma actuator. *Aerosp. Sci. Technol.* **2013**, *26*, 120–127. [CrossRef]
132. Zhang, Z.; Wu, Y.; Jia, M.; Song, H.; Sun, Z.; Li, Y. MHD-RLC discharge model and the efficiency characteristics of plasma synthetic jet actuator. *Sens. Actuators A Phys.* **2017**, *261*, 75–84. [CrossRef]
133. Moayedi, H.; Amanifard, N. Finding a low cost energy multi-DBD plasma actuator for natural heat transfer enhancement in a vertical duct. *J. Electrost.* **2020**, *108*, 103520. [CrossRef]
134. Mardani, A.; Khanehzar, A. Numerical assessment of MILD combustion enhancement through plasma actuator. *Energy* **2019**, *183*, 172–184. [CrossRef]
135. Massa, L.; Freund, J.B. Plasma-combustion coupling in a dielectric-barrier discharge actuated fuel jet. *Combust. Flame* **2017**, *184*, 208–232. [CrossRef]
136. Russo, N.; Gonzalez, L.M.; Viccione, G.; Pisacreta, C. A control mechanism of a typical fluid–structure interaction problem based on dielectric barrier discharge plasma actuation model. *Eur. J. Mech. B/Fluids* **2020**, *81*, 28–40. [CrossRef]
137. Abdollahzadeh, M.; Páscoa, J.; Oliveira, P. Two-dimensional numerical modeling of interaction of micro-shock wave generated by nanosecond plasma actuators and transonic flow. *J. Comput. Appl. Math.* **2014**, *270*, 401–416. [CrossRef]
138. Shang, J.; Huang, P. Surface plasma actuators modeling for flow control. *Prog. Aerosp. Sci.* **2014**, *67*, 29–50. [CrossRef]
139. Song, P.; Wu, Q.; Chen, L.; Wang, X.; Long, W. Numerical study on ionization characteristics of CH4/Air mixture employing plate dielectric barrier discharge. *Appl. Therm. Eng.* **2020**, *165*, 113573. [CrossRef]
140. Pescini, E.; Martínez, D.; De Giorgi, M.G.; Ficarella, A. Characterization of the effects of a dielectric barrier discharge plasma actuator on a coaxial jet in a Bunsen burner. *Exp. Therm. Fluid Sci.* **2018**, *91*, 292–305. [CrossRef]
141. Abdul Madhar, S.; Rodrigo Mor, A.; Mraz, P.; Ross, R. Study of DC partial discharge on dielectric surfaces: Mechanism, patterns and similarities to AC. *Int. J. Electr. Power Energy Syst.* **2021**, *126*, 106600. [CrossRef]
142. Foshat, S. Numerical investigation of the effects of plasma actuator on separated laminar flows past an incident plate under ground effect. *Aerosp. Sci. Technol.* **2020**, *98*, 105646. [CrossRef]